◆ Human Brain Mapping 6:216–238(1998) ◆

Spatio-Temporal Dynamics of Attention to Color: Evidence From Human Electrophysiology

Lourdes Anllo-Vento,[1]* Steven J. Luck,[2] and Steven A. Hillyard[1]

[1]*Department of Neurosciences, University of California, San Diego*
[2]*Department of Psychology, University of Iowa, Iowa City*

Abstract: This study characterized patterns of brain electrical activity associated with selective attention to the color of a stimulus. Multichannel recordings of event-related potentials (ERPs) were obtained while subjects viewed randomized sequences of checkerboards consisting of isoluminant red or blue checks superimposed on a grey background. Stimuli were presented foveally at a rapid rate, and subjects were required to attend to the red or blue checks in separate blocks of trials and to press a button each time they detected a dimmer target stimulus of the attended color. An early negative ERP component with an onset latency of 50 ms was sensitive to stimulus color but was unaffected by the attentional manipulation. ERPs elicited by attended and unattended stimuli began to diverge after approximately 100 ms following stimulus onset. Inverse dipole modelling of the attended-minus-unattended difference waveform indicated that an initial positive deflection with an onset latency of 100 ms had a source in lateral occipital cortex, while a subsequent negative deflection with an onset at 160 ms had a source in inferior occipito-temporal cortex. Longer-latency attention-sensitive components were localized to premotor frontal areas (onset at 190 ms) and to more anterior regions of the fusiform gyrus (onset at 240 ms). These source localizations correspond closely with cortical areas that were identified in previous neuroimaging studies as being involved in color-selective processing. The present ERP data thus provide information about the time course of stimulus selection processes in cortical areas that subserve attention to color. *Hum. Brain Mapping 6:216–238, 1998.*

Key words: ERP; dipole modelling; selection; features

INTRODUCTION

Recent accounts of visual perception and attention have emphasized that color is a highly effective cue for the identification and selection of relevant objects. Visual search studies, for example, have shown that a stimulus differing in color from homogeneous background items appears to pop out and can be detected effortlessly by the observer [Duncan and Humphreys, 1989; Theeuwes, 1990; Treisman and Gelade, 1980]. Similarly, human subjects are able to attend selectively to multifeature stimuli and identify changes in color apart from variations in other stimulus attributes [Garner, 1987; Theeuwes, 1996].

Studies of functional specialization in the primate brain have identified a neural pathway that encodes the wavelength changes associated with color perception, starting with color-opponent ganglion cells at the retinal level and reaching the blob regions of primary visual cortex (area V1) via the parvocellular layers of

Contract grant sponsor: NIMH; Contract grant number: MH-25594; Contract grant sponsor: NIH; Contract grant number: NS 17778; Contract grant sponsor: ONR; Contract grant number: N00014–93–1-0942.

*Correspondence to: Lourdes Anllo-Vento, Dept. of Neurosciences, University of California, San Diego, 9500 Gilman Dr., Dept. 0608, La Jolla, CA 92093–0608. E-mail: lanllo@ucsd.edu

Received for publication 27 January 1998; accepted 7 April 1998

the lateral geniculate nucleus [Livingstone and Hubel, 1984]. From V1, color information is relayed to extrastriate areas V2 and V4 and then to inferotemporal cortical regions [Komatsu et al., 1992; Schein and Desimone, 1990; Schiller et al., 1990]. Recent reviews of vision in primates have characterized the role of the occipitotemporal extrastriate pathway as broadly involved in the detailed feature analyses that lead to object identification and recognition [Heywood et al., 1992; Horel, 1994].

Lesions of inferior occipito-temporal cortex in humans are associated with a sensory impairment known as cerebral achromatopsia, which is characterized by an inability to perceive the color of objects [for reviews, see Damasio et al., 1980; Zeki, 1990]. The color deficits observed in achromatopsia are often accompanied by impairments of form perception, such as visual agnosia, but may also occur in the absence of significant form-related deficits. In accord with this evidence obtained from patients, recent brain-imaging studies have identified several areas of the human brain that are specifically responsive to the color of stimuli. In a positron emission tomography (PET) study, Zeki and his colleagues [Lueck et al., 1989; Zeki et al., 1991] presented subjects with colored and monochrome Mondrian stimuli and found that the colored stimuli elicited greater activation in a region of the lingual and fusiform gyri of the extrastriate cortex. Similarly, a recent study of a color aftereffect with functional magnetic resonance imaging (fMRI) reported activation of the posterior fusiform gyri of both hemispheres [Sakai et al., 1995]. Allison and collaborators [1993] used intracranial recordings of ERPs to show that this same general region of human inferior occipitotemporal cortex exhibited wavelength-specific adaptation effects. This color area occupied a segment of the inferior surface of the occipital and temporal lobes that included the medial and lateral aspects of the lingual gyrus, the posterior portion of the fusiform gyrus and, to a lesser extent, the inferior temporal gyrus.

Stimulus-elicited neural activity in these same cortical areas was found to be influenced by selective attention to color in a PET study by Corbetta and associates [1990, 1991]. When compared to the effects of dividing attention among multiple features, selective processing of stimulus color was associated with increased activation in the vicinity of the collateral sulcus, which separates the lingual and fusiform gyri, and in dorsolateral occipital cortex. The authors concluded that paying attention to a particular stimulus feature enhances neural activity in the specific cortical regions that encode that feature.

Despite increasing knowledge of the anatomical location of color-specific areas of the human brain, little information is available about the temporal characteristics of attentional selection within those areas. Such information is essential for understanding how sensory features such as color are encoded and selected in the brain, and for constraining cognitive models of attention. The timing of feature selection processes may be studied noninvasively in humans by recording ERPs from the scalp while subjects engage in attention-demanding tasks. By comparing ERPs elicited by stimuli when they are attended versus when they are not attended, it is possible to specify the timing of ERP components associated with feature-selective processing. In addition, by applying source localization techniques, it is possible to estimate the anatomical sources of the underlying neural activity.

The majority of ERP studies of selective attention have investigated spatial attention, that is the selection of a relevant location in the visual field. Spatial selective attention is associated with a characteristic pattern of ERP changes that includes amplitude enhancements of the early P1 (80–140 ms) and N1 (140–200 ms) components elicited by stimuli at attended locations [reviewed in Mangun and Hillyard, 1995]. The neural sources of the P1 and N1 spatial attention effects have been localized to specific regions of ventral and lateral extrastriate visual cortex by means of scalp current density (SCD) mapping and inverse dipole modelling techniques [Clark and Hillyard, 1996; Gomez Gonzalez et al., 1994; Mangun et al., 1993; Simpson et al., 1995]. In addition, by combining ERP recordings with PET neuroimaging, it has been possible to specify both the timing and anatomical location of stimulus selection processes during spatial attention [Heinze et al., 1994; Mangun et al., 1997; Woldorff et al., 1997]. The pattern of P1 and N1 amplitude enhancements associated with spatial attention is very different from the later ERP modulations associated with attention to nonspatial stimulus features such as color [Anllo-Vento and Hillyard, 1996; Hillyard and Münte, 1984; Karayanidis and Michie, 1996; Smid and Heinze, 1997; Wijers et al., 1989], orientation [Harter and Guido, 1980; Kenemans et al., 1993; Rugg et al., 1987], or spatial frequency [Harter and Previc, 1978; Heslenfeld et al., 1997; Kenemans et al., 1993; Previc and Harter, 1982; Zani and Proverbio, 1995]. Stimuli that are selected on the basis of these nonspatial cues generally elicit broad ERP deflections over the interval 150–350 ms poststimulus, including posterior "selection negativity" (SN) and anterior "selection positivity" (SP) components [Anllo-Vento and Hillyard, 1996; Harter and Aine, 1984].

To our knowledge no studies have yet attempted to localize the anatomical sources of the ERPs associated with attention to non-spatial features such as color, nor to relate those sources to the cortical areas shown by previous neuroimaging studies to be responsive to

color. The present study undertook such an analysis, with the aim of defining both the spatial-anatomical and temporal characteristics of neural activity subserving attention to color. In the present design, multichannel recordings of ERPs were obtained from subjects who attended selectively to either red or blue checkerboard patterns presented in a random sequence. ERP components associated with color-selective attention were isolated by subtracting the ERP elicited by a given color when it was not attended from the ERP elicited by the same color when it was attended. The locations of the cortical generators of these ERP color-attention effects were estimated by inverse dipole modelling using the Brain Electrical Source Analysis (BESA) algorithm [Scherg, 1990].

Because inverse modelling techniques such as BESA do not generally yield unique solutions with respect to ERP sources, several aspects of the present experimental design were aimed at enhancing the validity of this localization procedure. First, a large number of trials was presented to achieve high signal-to-noise ratios in the ERP averages. Second, dipole source localization was performed on attended-minus-unattended difference waveforms rather than on the original ERP waveforms, thus decreasing the number of simultaneously active ERP sources and simplifying the dipole analysis. Third, dipole localization was carried out separately for two independent sets of trials (standard and target stimuli) thereby testing the stability of the calculated source locations. Fourth, several different strategies for fitting the multiple dipoles to the observed ERP distributions were compared in order to assess possible errors in the inverse modelling procedure. Finally, structural magnetic resonance imaging (MRI) scans were obtained for six of the subjects in the study, making it possible to localize the ERP sources in the standard Talairach coordinate system and to compare their locations with the results of previous functional imaging research. By demonstrating a close correspondence between the calculated dipole locations and the anatomical areas that showed color-specific activation in prior neuroimaging studies, the validity of the calculated dipole models could be substantiated and inferences could be made about the timing of color-selective processing during attention in each of the participating cortical areas.

METHODS

Subjects

Sixteen right-handed volunteers (10 females) between the ages of 19 and 31 (average age = 22 years) were paid for their participation in this experiment. Subjects reported having normal or corrected-to-normal visual acuity and normal color vision.

Stimuli and task

The stimuli consisted of red-and-grey and blue-and-grey checkerboards, which were presented for a duration of 100 ms against a constant grey background on a high-resolution computer screen (see Fig. 1). The checkerboards subtended 4.8° × 4.8° of visual angle at a viewing distance of 70 cm and were centered at the fovea. Check size was 0.6°. Red and blue checkerboards were presented in random order with stimulus onset asynchronies (SOAs) that varied randomly between 150 and 450 ms.

For the frequently presented standard stimuli (P = .90), the x and y CIE (Commission International d'Eclairage) coordinates were x = 0.437 and y = 0.308 for the red, and x = 0.162 and y = 0.102 for the blue checks. The red and blue checks were equated for brightness (at a luminance level of approximately 9.8 cd/m^2) by minimizing heterochromatic flicker in tests carried out on two color-normal experimenters. The grey background and grey checks (x = 0.250, y = 0.244) had a luminance level of 7.4 cd/m^2. The infrequent target stimuli (P = .10) were identical to the standard checkerboards except for a slight decrease in the luminance of the red or blue checks, which made them appear dimmer than the standards. All four types of stimuli were combined in randomized sequences, with a different random ordering for each 4-min block of trials.

At the beginning of each of the 12 blocks comprising the experiment, one of the two colors was designated to be attended, and the subject was instructed to respond with a button press each time a dimmer target of the attended color was detected. Equal numbers of attend-red and attend-blue blocks were run in counterbalanced order. The luminance of the target checks was adjusted separately for each subject to maintain a consistent performance level of 70–80% correct detections throughout the experiment.

ERP recordings and analysis

The EEG was recorded from 32 electrodes, including 17 sites from the 10–20 system (F3, F4, F7, F8, C3, C4, P3, P4, O1, O2, T3, T4, T5, T6, Fz, Cz, and Pz), the left mastoid, and 12 additional electrode sites covering the posterior one-third of the scalp (see below), all referenced to the right mastoid. Bipolar recordings from the left and right outer canthi were used to measure horizontal eye movements, and blinks were recorded from an electrode placed below the left eye and

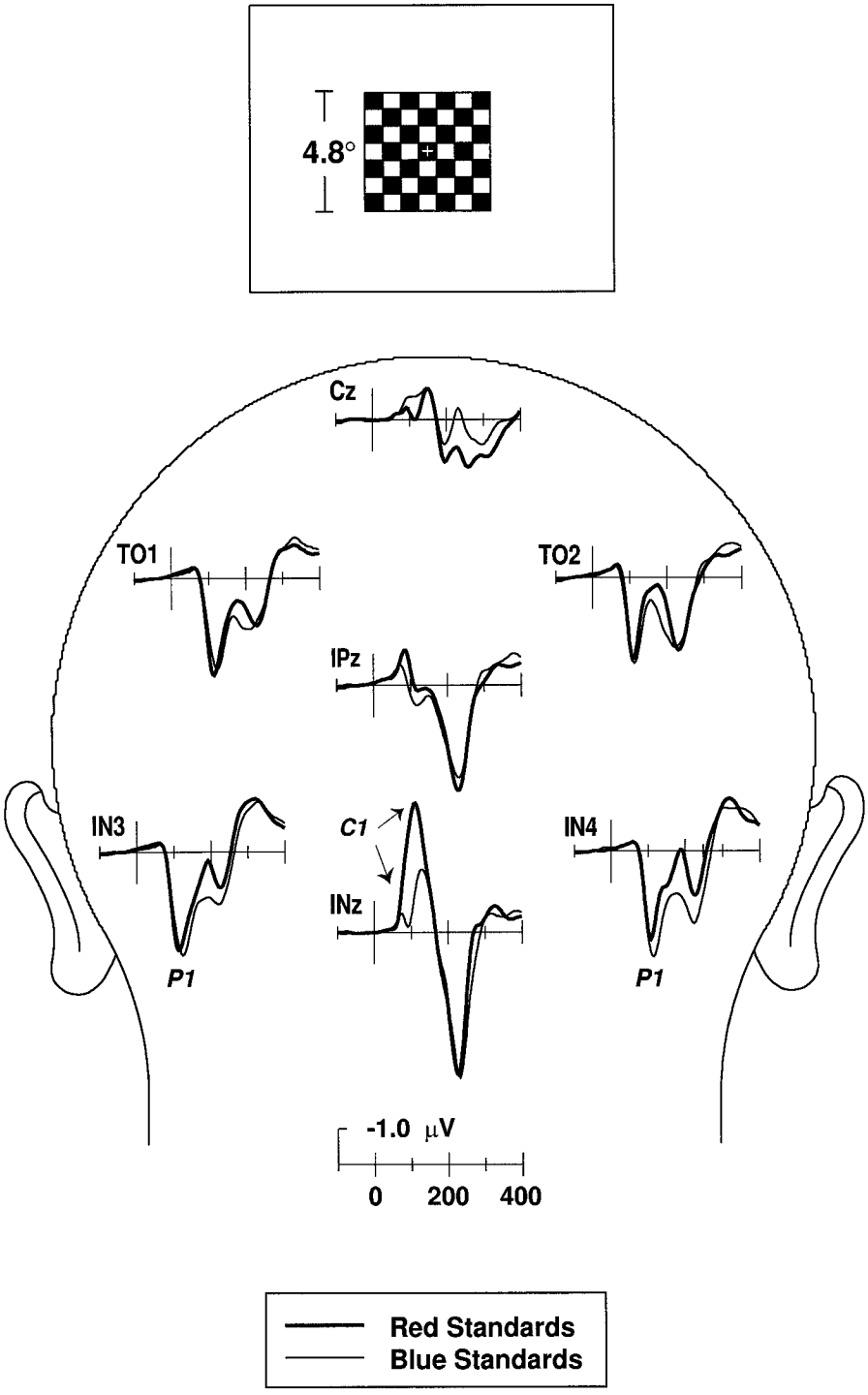

Figure 1.
Grand-average ERPs over 16 subjects in response to red and blue standard (nontarget) checks. Waveforms from seven representative scalp sites are averaged across attend-red and attend-blue conditions.

referred to the right mastoid. The EEG was amplified with a bandpass of 0.01–100 Hz (half-amplitude cutoffs) and digitized at a sampling rate of 250 Hz. Trials with artifacts (e.g., blinks, eye movements, amplifier saturation) were rejected off-line during signal averaging. After artifact rejection, the mean number of standard-stimulus trials included in each averaged ERP waveform for each subject in each condition was 4,425.

Because of the short interstimulus intervals used in this study (150–450 ms), the ERP waveforms elicited by successive stimuli overlapped in time, leading to distortions in the ERP averages. Accordingly, the AD-

JAR procedure developed by Woldorff [1993] was used to remove the estimated overlap from ERP waveforms. This procedure required digital high-pass filtering of the waveforms with a causal filter (50% amplitude cutoff at 0.02 Hz). The absence of significant ERP activity in the baseline prior to stimulus presentation is indicative of successful overlap removal (see Fig. 1).

Separate averages were calculated for ERPs to standard and target stimuli of each color under each attention condition (i.e., red attended, red unattended, blue attended, and blue unattended). All waveform measurements were performed after the waveforms were algebraically re-referenced to the average of the two mastoids in order to avoid hemispheric biases. Mean amplitudes of the main ERP components were calculated within specified time windows (see Table I), both for the original waveforms and for the attentional difference waves (i.e., waveforms that were obtained by subtracting the response to the unattended stimuli from the ERP to the same stimuli when they were being attended). The presence of color attention effects was demonstrated by testing the amplitude of the ERP components in the attentional difference waves against zero using repeated measures ANOVAs. An initial ANOVA that included stimulus color (red vs. blue) and scalp site as factors revealed no significant effect of specific color on the amplitude of any attentional difference wave components; accordingly, ERPs were combined across stimulus color for the analyses reported here. Each amplitude measure was initially subjected to an ANOVA which included all electrode locations; subsequent ANOVAs were used for a subset of electrodes only when the initial analysis revealed significant interactions between the attention and electrode site factors. All statistical analyses including more than two electrode locations included the Greenhouse-Geisser sphericity correction [Vasey and Thayer, 1987]. In addition, all comparisons of ERP scalp distributions across experimental conditions were scaled to a common amplitude according to the procedure of McCarthy and Wood [1985].

Modelling of ERP sources

Maps of voltage topography and SCD [Perrin et al., 1989] were calculated for the major components of the attentional difference waves. These topographical maps identify areas where current flows in or out of the scalp [Nunez, 1981] and provide qualitative information about the number of generators and their likely orientation. Due to mathematical constraints on the computation of spline maps [Perrin et al., 1989], the right mastoid was used as the unique reference site in calculating topographical maps.

The three-dimensional positions of the recording electrodes were determined by means of a Polhemus Isotrak digitizer for 12 of the 16 subjects in this study. This procedure involved stabilizing the subject's head with a bite-bar and recording the three-dimensional coordinates of three fiducial landmarks (nasion, and left and right preauricular points) and each electrode location. The coordinates thus obtained were used to calculate the best-fitting sphere that encompassed each subject's electrode locations.[1] The average spherical electrode coordinates for these 12 subjects (given in Table II) were used in plotting the topographical maps of the group's average waveforms and in modelling the dipolar sources.

Inverse source analyses of the attentional difference waves were performed using the commercially available BESA software (Version 2.0). The BESA algorithm estimates the location and orientation of multiple equivalent dipolar sources by calculating the scalp distribution that would be obtained for a given dipole model (the "forward solution") and comparing it to the original ERP distributions. Iterative changes in the location and orientation of the dipole sources lead to minimization of the residual variance (RV) between the model and observed spatiotemporal ERP distributions [Scherg, 1990]. The energy criterion of the BESA program was set at 20% to reduce interactions among dipoles, and the separation criterion was set at 10% to optimize the separation of source waveforms that differ over time. In these calculations, BESA assumed an idealized spherical head model of 85 mm radius (corresponding well with the mean measured radius of 84 $\pm$ 3 mm in our group), and scalp and skull thicknesses of 6 and 7 mm, respectively.

Anatomical localization of dipolar sources

The MRIs of six subjects were obtained according to the following protocol: A 1.5 Tesla GE Signa MRI scanner was used with a quadrature head coil. The subject's head was stabilized by means of foam pads and surgical tape. A short T1-weighted localizer sequence in the saggital plane was followed by a high-resolution T1 weighted spoiled GRASS (SPGR) sequence in the axial plane (repetition time (TR) = 24 ms; echo time (TE) = 6 ms; 1 excitation (NEX); field of view (FOV) = 24 cm; matrix = 256X256; thickness = 1.1

[1] We calculated the best-fit sphere for each subject as well as the amount of error between each electrode position and the spherical surface. The most discrepant sites (T3 and T4) were routinely omitted from the calculation of the sphere in order to reduce the average error.

TABLE I. Measurement windows and electrode sites for major ERP components in this study

Component	Latency (ms)	Electrode sites measured
Standard stimuli		
C1	50–90	Fz, Cz, Pz, IPz, INz
PD130	100–140	O1/O2, IN3/IN4, T5/T6, TO1/TO2, P3/P4, PO1/PO2
SN	160–250	O1/O2, IN3/IN4, T5/T6,
	250–325	TO1/TO2
SP	180–230	F3/F4, F7/F8, C3/C4, CT5/CT6, T3/T4, CP1/CP2
Target stimuli		
PD130	115–160	O1/O2, IN3/IN4, T5/T6, TO1/TO2, P3/P4, PO1/PO2
SN	168–250	O1/O2, IN3/IN4, T5/T6,
	250–325	TO1/TO2
SP	180–230	F3/F4, F7/F8, C3/C4, CT5/CT6, T3/T4, CP1/CP2
P3	325–600	All scalp electrodes

mm). This SPGR protocol provided near equal resolution in all three planes. The exact FOV and thickness were varied across subjects in order to optimize the imaging volume.

The axial MRI images were used to compute a three-dimensional volume, which could be imaged in the axial, coronal, or saggital planes. The locations of the cranial fiducial landmarks (left and right preauricular points, and nasion) were identified in the MRIs to enable the transformations required for co-registering the spherical coordinates of the calculated dipoles and the three-dimensional coordinates of the MRI scans [Towle et al., 1993].

In order to estimate the positions of the dipole sources with respect to brain anatomy, the dipole coordinates calculated from the group average ERP distributions were projected onto the MRIs of individual subjects [Giard et al., 1994; Pantev et al., 1995], and the corresponding regions were identified on standard atlases [Damasio, 1995; Talairach and Tournoux, 1988]. Because of individual variations in the geometrical relationship between brain and skull anatomy, a more valid estimate of average dipole locations within the group was obtained by averaging the anatomical coordinates of each dipole across the six individuals whose MRIs were available. The line between the anterior (A) and posterior (P) commissures was identified on each subject's MRI scan as the principal A-P axis for the Talairach and Tournoux [1988] coordinate system, and the three-dimensional coordinates of each dipole in the group-average BESA model were determined on the MRI with respect to the Talairach axes, scaled according to brain size. The mean values of the Talairach coordinates of each dipole were calculated over the six subjects and were taken as estimates of the average anatomical position

TABLE II. Spherical angles for standard BESA and observed group-average electrode sites*

Standard BESA sites			Group average sites		
Electrode	Theta	Phi	Electrode	Theta	Phi
F3	−62	−57	F3	−53	−58
F4	62	57	F4	52.5	54.3
F7	−90	−36	F7	−80	−43
F8	90	36	F8	80.6	39.9
C3	−45	0	C3	−38	−5.5
C4	45	0	C4	37.7	2.6
P3	−62	57	P3	−50	50.7
P4	62	−57	P4	50.7	−53
O1	−90	72	O1	−79	73.6
O2	90	−72	O2	78.9	−78
T3	−90	0	T3	−80	−3.4
T4	90	0	T4	79.5	−0.2
T5	−90	36	T5	−79	37.4
T6	90	−36	T6	79.9	−41
CP1	−30	45	CP1	−24	46.9
CP2	30	−45	CP2	25.2	−48
CT5	−71	18	CT5	−59	18.3
CT6	71	−18	CT6	58.8	−21
PO1	−68	76	PO1	−59	76.3
PO2	68	−76	PO2	58.1	−80
TO1	−84	55	TO1	−71	55.2
TO2	84	−55	TO2	71.2	−60
IN3	−109	55	IN3	−103	56.1
IN4	109	−55	IN4	102	−62
Fz	45	90	Fz	41.3	88.1
Cz	0	0	Cz	0	0
Pz	45	−90	Pz	−40	87.3
Ipz	77	−90	IPz	−69	87.1
INz	109	−90	Inz	−100	88.8
LM	−118	10	LM	−127	17.6
RM	118	−10	RM	128	−19

* Theta: angle from the superior-inferior Z axis (through Cz); Phi: angle from X axis parallel to the line between left and right preauricular points in the X-Y plane. The Y axis passes through FPz and Oz. Positive values of theta denote the right side of scalp and negative values denote the left side. Positive values of phi are measured counterclockwise and negative values are measured clockwise from the X axis. LM and RM refer to left and right mastoids, respectively.

of each dipole generator source for the group [Clark and Hillyard, 1996].[2]

RESULTS

Behavioral performance

Hits were defined as responses to target stimuli of the attended color with reaction times between 200 and 1,000 ms after stimulus onset. Percent hits averaged 77.7% for red checks and 78.5% for blue checks. False alarm rates were calculated as the percentage of standards of the attended color that was followed by a response (Red = 3.4%; Blue = 3.6%) and, alternatively, as the percentage of targets of the unattended color that was followed by a response (Red = Blue = 5.2%). In neither case was there a significant difference in performance between colors. Reaction times were also comparable when responding to red and blue checks (Red = 513 ms; Blue = 508 ms).

Event-related potentials

Figure 1 compares ERPs elicited by red and blue standard checks averaged across attention conditions. The earliest component was a sharply focused posterior midline negativity onsetting at 50 ms that was labelled C1, following the terminology of Jeffreys and Axford [1972]. The C1 waveforms differed according to stimulus color, with the red checks eliciting a single large peak at a mean latency of 107 ms and the blue checks a double-peaked waveform with peaks at 72 ms and 128 ms. There was also a difference in midline scalp topography of the early phase of the C1 (quantified as the mean amplitude over 50–90 ms) in response to the red and blue checks (color x electrode site: $F(4,60) = 6.17$, $P < 0.01$), reflecting a more inferior amplitude maximum in the scalp distribution of the C1 to the red checks (Fig. 2).

Although the early ERP waveforms differed between the two colors, the effects of attention on the ERPs to the red and blue checks did not differ significantly. Therefore, the attention effects were analyzed for ERP waveforms averaged over red and blue stimuli. As shown in Figure 3, the C1 at midline posterior sites was not affected by the attentional manipulation in the latency range 50–150 ms ($F[1,15]<1$).

[2] A modelling study by Clark [1993] supports the validity of estimating average dipole positions in a subject population on the basis of inverse dipole analysis of the grand-average waveforms over all subjects. Further justification for the procedure is presented in Clark and Hillyard [1996].

At posterior lateral sites, the C1 was paralleled by a positive P1 component, which peaked at 119 ms with a maximum amplitude over inferior occipito-temporal regions (Figs. 1 and 2). The earliest attention effect occurred during the time-range of the P1 component, with a slightly greater positivity elicited by stimuli of the attended color. Following the P1, the attended ERPs showed a sustained negativity relative to the unattended ERPs over posterior sites (Fig. 3). These and other attention effects can be more clearly observed in Figure 4, which shows difference waves obtained by subtracting the ERPs to checks of the unattended color from the ERP response to the same color checks when attended.

Attentional difference waves: Standard stimuli

The initial positive deflection in the difference waves had its onset at about 100 ms and a peak latency of 130 ms; this positive difference (PD130) was quantified as the mean amplitude over the interval 100–140 ms (Table I). The PD130 was significantly greater than zero over posterior electrode sites ($F[1,15]=8.84$, $P < 0.01$) and was nonsignificantly larger over the left hemisphere (Fig. 5).

The PD130 in the attentional difference waves was followed by a broad negative deflection over the posterior scalp, which began at about 160 ms, peaked at 220–240 ms, and continued until about 350 ms. This ''selection negativity'' (SN) was accompanied by an anterior ''selection positivity'' (SP) that peaked at about 210 ms and continued until about 250 ms. The voltage and SCD distributions of the SP and the early and late phases of the SN are shown in Figure 5.

The SN was quantified as the mean amplitude of the attentional difference wave in its early (160–250 ms) and late (250–325 ms) phases at occipital and temporal electrode sites (Table I). The effect of attention on the early phase of the SN was highly significant ($F[1,15] = 21.73$, $P < 0.001$) and was larger over medial (O1/O2) and inferior (IN3/IN4) occipital electrodes than over lateral temporal (T5/T6) and occipito-temporal (TO1/TO2) sites (electrode site: $F(3,45) = 27.03$, $P < 0.001$). The later phase of the SN was also significantly greater than zero ($F(1,15)=25.71$, $P < 0.001$) but showed a slightly more inferior and lateral distribution than the earlier phase when the two intervals were included in a combined analysis (time interval x electrode site: $F(3,45) = 7.37$, $P < 0.001$).

The anterior SP was quantified as the mean amplitude of the attentional difference wave between 180 and 230 ms over frontal and central sites. The SP was significantly greater than zero ($F(1,15) = 28.26$, $P < 0.001$) over the central and anterior scalp (electrode

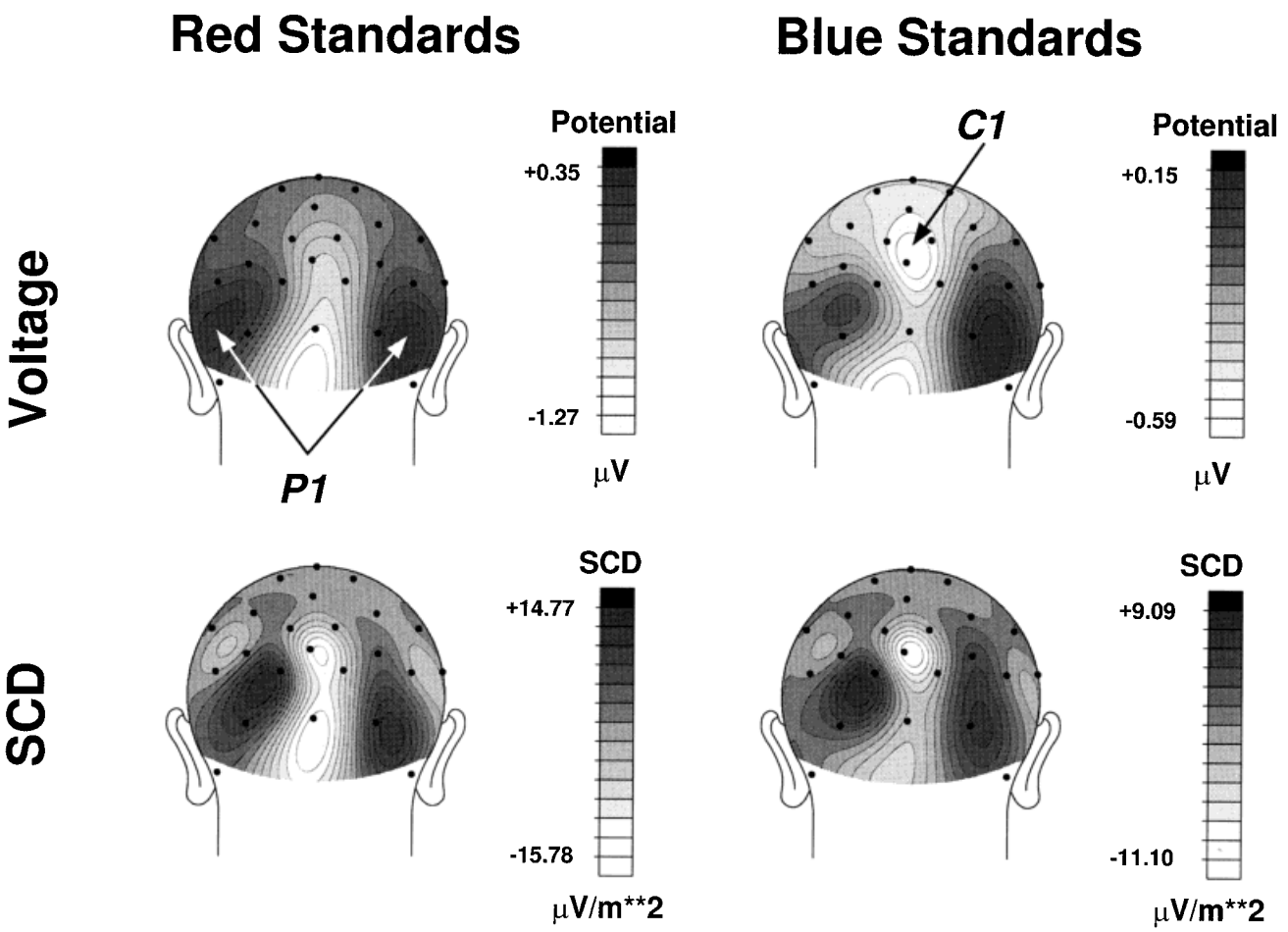

Figure 2.
Spline-interpolated topographical maps of voltage (**top row**) and scalp current density (SCD; **bottom row**) of the C1 component (measured over 50 to 90 ms) of the VEP evoked by red (**left**) or blue (**right**) standard stimuli.

site: $F(5,75) = 9.56$, $P < 0.001$) and was larger over the left hemisphere at central sites (electrode site x hemisphere: $F(5,75) = 4.45$, $P < 0.003$; Fig. 5).

Attentional difference waves: Target stimuli

Difference waves generated by subtracting the unattended target from the attended target ERPs revealed similar patterns of attentional modulation (Fig. 6), though the onset latencies of the PD130, SN, and SP were slightly delayed with respect to those of the standards, probably because of the lower luminance of the targets (Table I). These components of the attentional difference waves were larger in amplitude for the target than for the standard difference waves and were followed by a large P3 component. Figure 7 shows the topographical distributions of voltage and SCD of the attentional difference components elicited by target stimuli, which strongly resembled those elicited by standards (Fig. 5).

As in the case of the standard stimuli, the earliest target attention effect was a greater positivity (PD130, 115–160 ms) in response to targets of the attended color compared to targets of the unattended color ($F(1,15) = 12.7$, $P < 0.003$), and this effect was larger for target than for standard stimuli (stimulus type: $F(1,15) = 5.10$, $P < 0.04$). The target SN was also larger than the standard SN (stimulus type: $F(1,15) = 26.37$, $P < 0.001$) but showed a similar pattern of attentional modulation. The early phase of the target SN (175–250 ms) was significantly greater than zero ($F(1,15) = 4.84$, $P < 0.05$) and was larger at occipital electrodes (O1/O2 and IN3/IN4) than at occipito-temporal sites (TO1/TO2; electrode site: $F(2,30) = 28.91$, $P < 0.001$).

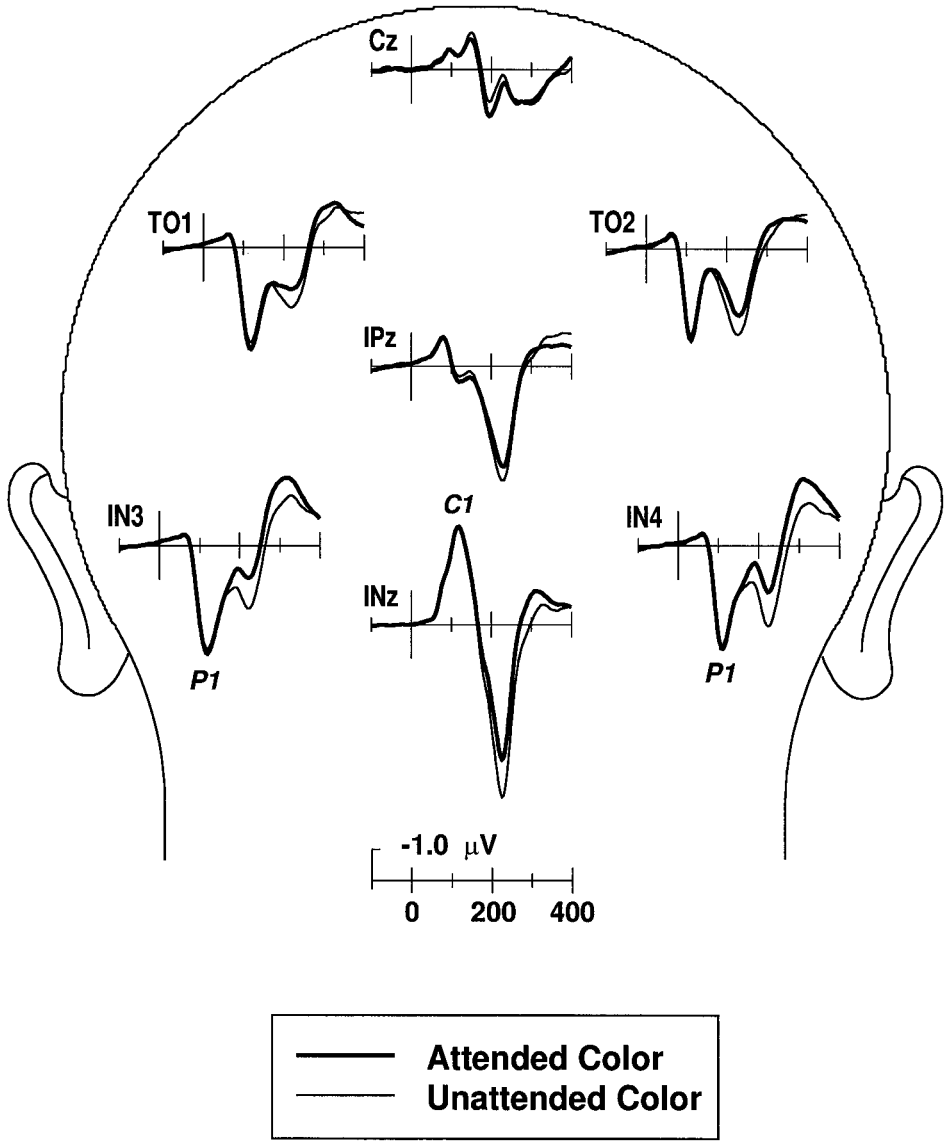

Figure 3.
Grand-average ERPs in response to standard checks of attended and unattended colors, averaged across red and blue checks.

The later phase of the SN (250–325 ms) was also significant ($F(1,15) = 25.71$, $P < 0.001$) and had a more lateral and inferior distribution than the early phase of the SN (time interval × electrode site: $F(3,45) = 3.03$, $P < 0.04$), as in the case of the standard stimuli. Finally, the target SP was also significantly greater than zero ($F(1,15) = 33.45$, $P < 0.001$) and was larger for target than for standard stimuli (stimulus type: $F(1,15) = 17.62$, $P < 0.001$). The target SP showed the same pattern of hemispheric lateralization as the SP to the standard stimuli, with a small but significant left-hemisphere dominance over central-medial sites (electrode site × hemisphere: $F(5,75) = 3.33$, $P < 0.03$).

The target difference waves were also characterized by a prominent and broadly distributed P3 component with an onset about 300 ms poststimulus and a peak latency of 488 ms. The P3, measured as the mean amplitude over 325–600 ms at all scalp electrodes, was significantly enhanced by attention ($F(1,15) = 57.92$, $P < 0.001$) and was largest over medial parietal regions (electrode site: $F(28,420) = 28.16$, $P < 0.001$).

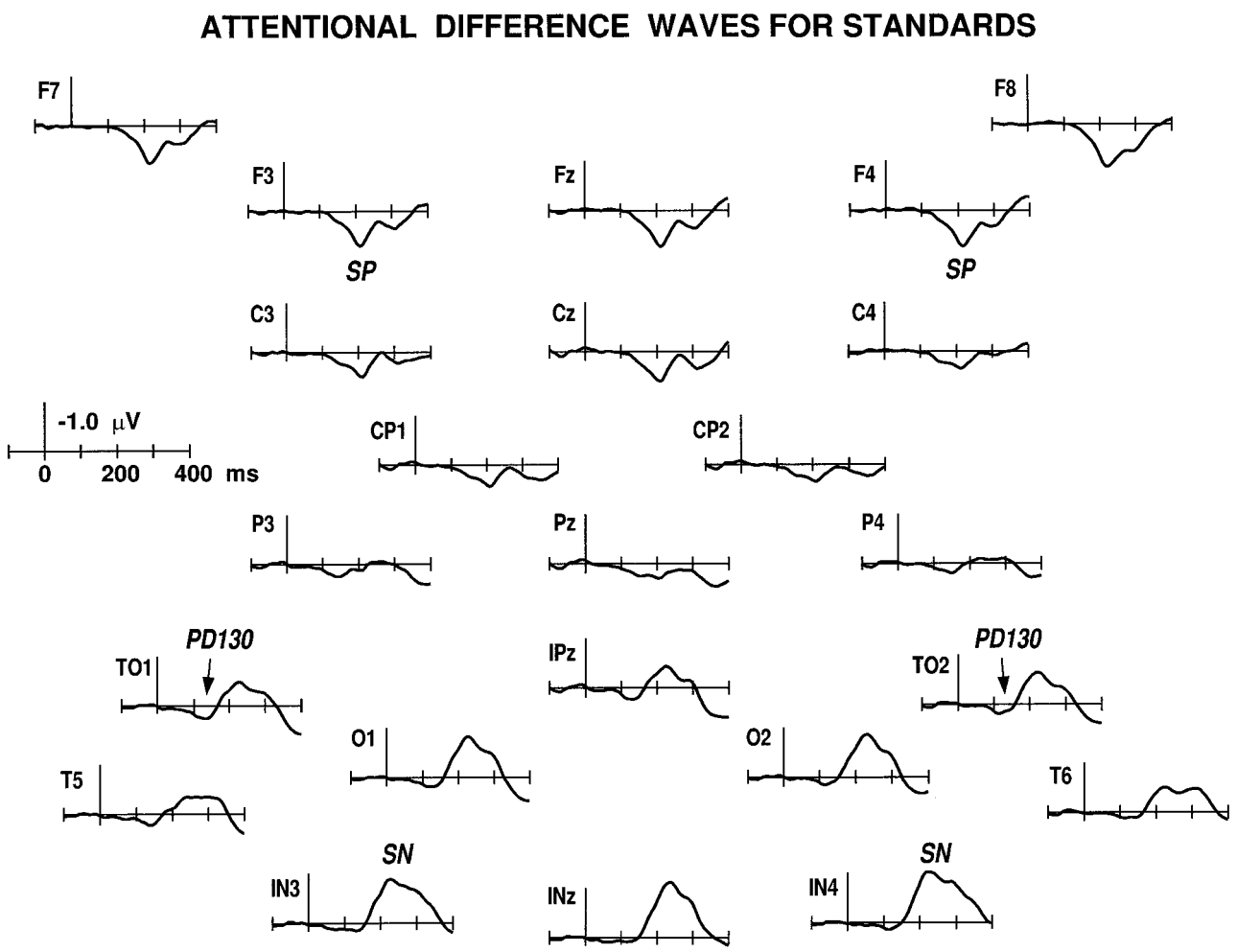

Figure 4.
Grand-average difference waves associated with selection of the attended color standards, obtained by subtracting average ERPs to standard color checks when unattended from the same color checks when attended. Difference waves to red and blue stimuli are averaged together.

Dipole source modelling

The voltage topography of the grand average attentional difference wave for standard stimuli was fit with multiple dipoles over the interval 100–325 ms. Principal component analysis (PCA) was employed to estimate the minimal number of dipoles that should be included in the model. A single value decomposition of the 225-ms epoch indicated that four principal components were needed to explain 99% of the variance in the data. Since the stimuli were foveally presented and the topographical distribution of the difference waves was generally bilaterally symmetrical, four dipole pairs were fitted in turn, with the locations and orientations of the two dipoles in each pair constrained to be mirror-symmetrical. A sequential strategy was used whereby one pair of mirror-symmetrical dipoles was fit at a time over successive time intervals. In each case several different starting dipole positions were used and a dipole solution was accepted only if it could be achieved from these various starting points. The interval for fitting each dipole pair was determined by considering the component structure and topography of the attentional difference waveform between 100 and 325 ms, as follows:

The first dipole pair was fit over the 100–140 ms interval corresponding to the initial positive modulation of the attentional difference wave, PD130 (Figs. 4 and 5). A stable solution was obtained that accounted for 82% of the variance within that interval. While

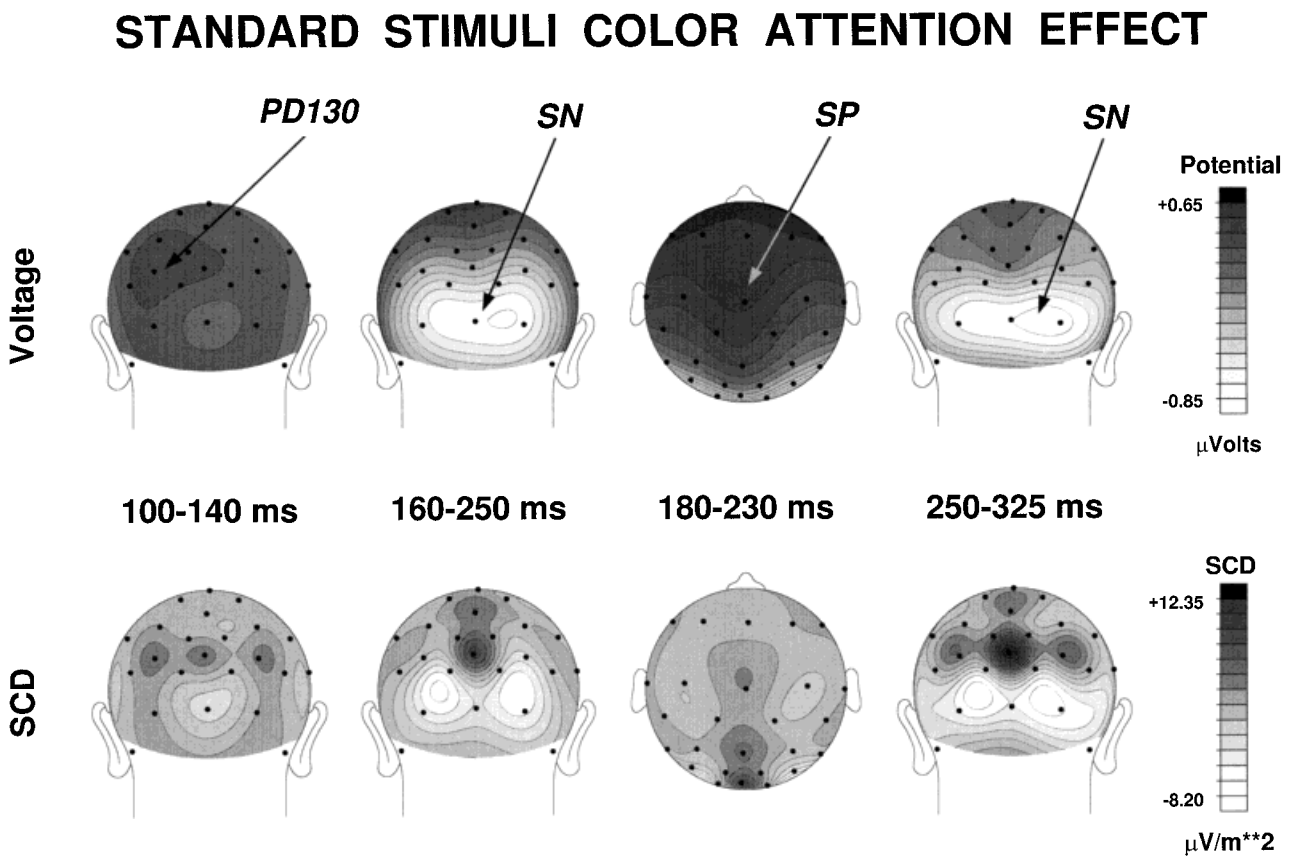

Figure 5.
Spline-interpolated topographical maps of voltage (**top row**) and scalp current density (**bottom row**) of the major components of the attentional difference waves depicted in Figure 4. Components were measured as mean amplitudes over the indicated intervals.

leaving this first dipole pair in place, a second pair of dipoles was then added to fit the early portion of the SN between 160 and 215 ms. This second dipole pair, together with the one previously fit, accounted for 98.5% of the variance present in the 100–215 ms interval and appeared to account for both the posterior SN and part of the anterior SP effects. An additional portion of the SN/SP was modelled by a third dipole pair over the interval between 190 and 240 ms, with the first two dipole pairs held constant. The addition of this third dipole pair reduced the RV to less than 1% in the interval between 100 and 240 ms, but this six-dipole model showed diminished adequacy beyond 240 ms. Accordingly, a fourth pair of dipoles was needed to provide an adequate and stable fit for the SN over the 240–320 ms interval. The process of fitting each dipole pair in sequence was reiterated until the RV was minimized and dipoles were stable in location and orientation. It should be noted, however, that reiterations beyond the initial dipole fit had little influence on the locations and orientations of the dipoles in the model.[3]

[3] In order to assess possible sources of error that might have been introduced by the sequential dipole fitting procedure that was used in our main analysis, several alternative fitting strategies were also evaluated. First, dipoles 1 and 2 were fit with the bilateral symmetry constraint relaxed, since the voltage topography of the PD130 was clearly asymmetrical. With both location and orientation symmetry constraints relaxed, the calculated positions of dipoles 1 and 2 were shifted by 6.7 and 6.4 mm, respectively, from the original model. Second, dipolar sources 3 and 4 were modelled with and without fitting the initial activity in the 100–140 ms interval. The distance between the dipolar pair for the initial phase of the selection negativity (160–215 ms) without any previous sources and the corresponding dipole pair (dipoles 3 and 4) in the original model was 7.7 mm. Third, we evaluated the effect of fitting dipole pairs 1–2, 3–4, and 5–6 simultaneously rather than sequentially within the interval 100–228 ms. Using the dipole positions of the original model as a starting point, simultaneous fitting resulted in a new model with locations of the three dipole pairs shifted by 2, 5, and 12 mm,

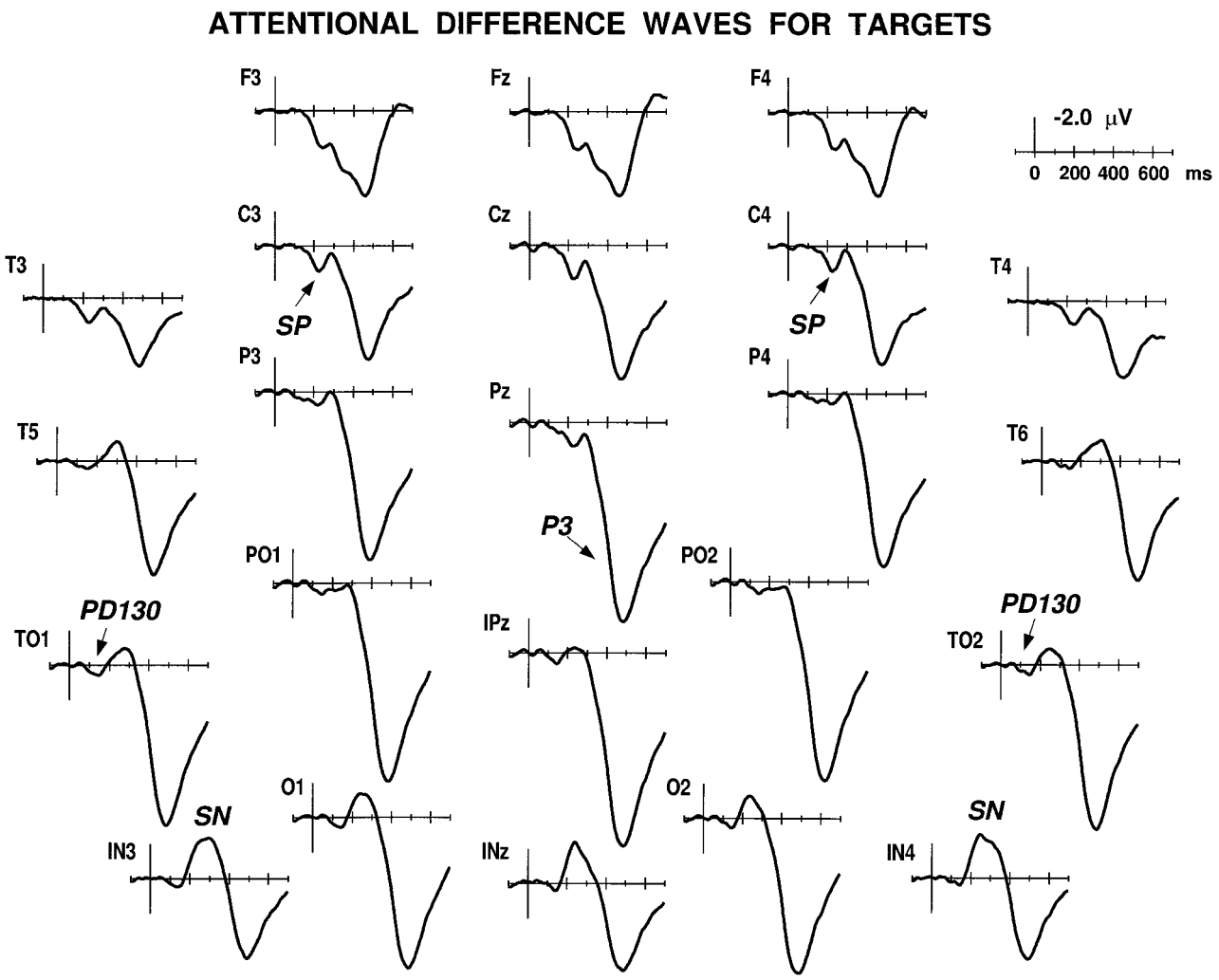

Figure 6.
Grand-average difference waves associated with selection of the dimmer targets of the attended color, obtained by subtracting ERPs to dimmer target checks of the unattended color from the same target checks when attended. ERPs from 23 representative electrode sites are shown.

Figure 8 shows the final eight-dipole model that accounted for 98.6% of the variance in the scalp distribution of the attentional difference wave elicited by the standard checks over the 100–325 ms interval. Note that the source waveforms for the first dipole pair (dipoles 1 and 2) correspond in time course and topographical distribution (Figs. 4 and 5) to the initial PD130 attentional effect, as well as a small early portion of the SN. The second dipole pair (dipoles 3 and 4) accounted for most of the symmetrical SN effect and much of the anterior SP, thus suggesting that SN and SP share, at least in part, common generator sources. Dipoles 5 and 6 accounted for a later, asymmetrical portion of the SN/SP, while dipoles 7 and 8 corresponded to the later portion of the SN that was shifted anteriorly and laterally as described above.

To assess interindividual variability in the localization of the principal dipolar sources (i.e., dipoles 3 and 4) in this model, the early portion of the SN was fit separately for each of the 12 subjects in the study for whom digitized electrode locations were available. Each subject's electrode locations and best-fit spherical

respectively. However, since this simultaneous fitting procedure does not take into account the time course and voltage topography of the ERP attention effects, we have more confidence in the original sequential approach. In any case, the different modelling strategies all yielded dipole arrays that did not differ markedly from those of the original model.

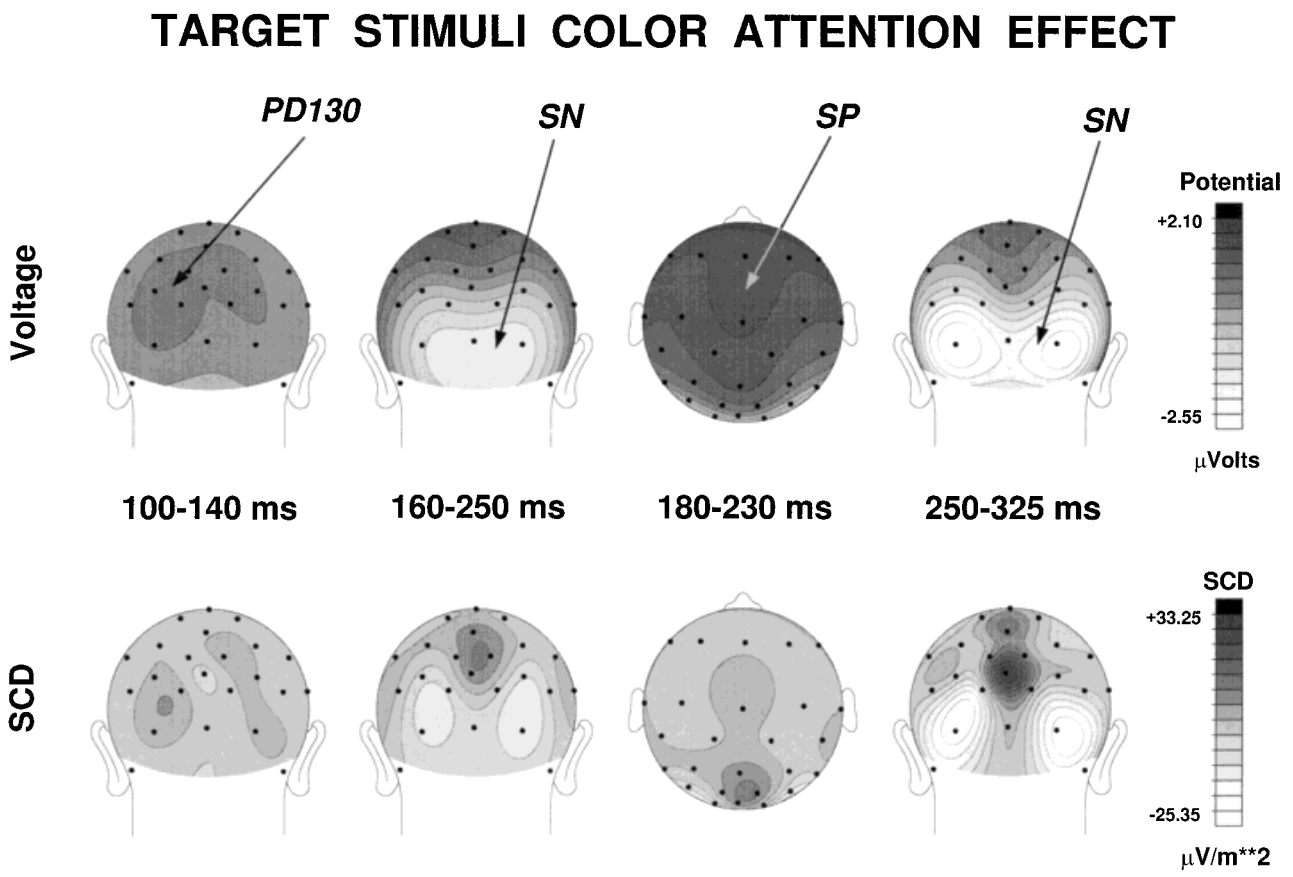

Figure 7.
Spline-interpolated topographical maps of voltage (**top row**) and scalp current density maps (**bottom row**) of the major components of the target difference waves depicted in Figure 6.

radius were used in modelling the location and orientation of the dipole pair accounting for the initial portion of the SN (160–215 ms) to standard stimuli. Figure 9 shows the locations and orientations of the individual dipoles as well as the location and orientation of dipoles 3 and 4 for the grand-average model in Figure 8.

On the average, the individually fitted dipole pair accounted for 92.75% (SD = 3.2%) of the variance in the 160–215 ms interval. These individual dipoles formed a relatively compact cluster and their mean location was quite close to that of the grand average model dipole (9 mm difference).

The dipole model obtained for the standard difference waves (Fig. 8) also provided a good fit to the difference waves for the target stimuli, accounting for 92.6% of the variance in those data. Moreover, the source waveforms corresponding to the dipoles in the target difference waves closely resembled those obtained for the standard stimuli. Nevertheless, the goodness-of-fit of the model could be further improved either by re-fitting the last pair of dipoles while keeping the rest of the model fixed (RV=1.3% [100–325 ms]) or by adjusting the orientations of the four dipole pairs in sequence (RV = 1.4%).

To further evaluate this apparent similarity of the dipolar sources of the standard and target attention effects, a separate model was fit to the target difference wave, taking the standard model as a point of departure. Since the target difference waves showed slight delays in onset latency with respect to their standard counterparts, the PD130 effect was modelled between 112 and 155 ms, and the SN was fit starting at 168 ms. The third pair of dipoles, however, appeared to have the same onset latency that was observed for the standards and was modelled between 190 and 250 ms. Finally, the fourth pair of dipoles was fit between 250 and 325 ms. The final eight-dipole model for the target difference waves explained 99% of the variance between 100 and 325 ms. Table III gives the parameters

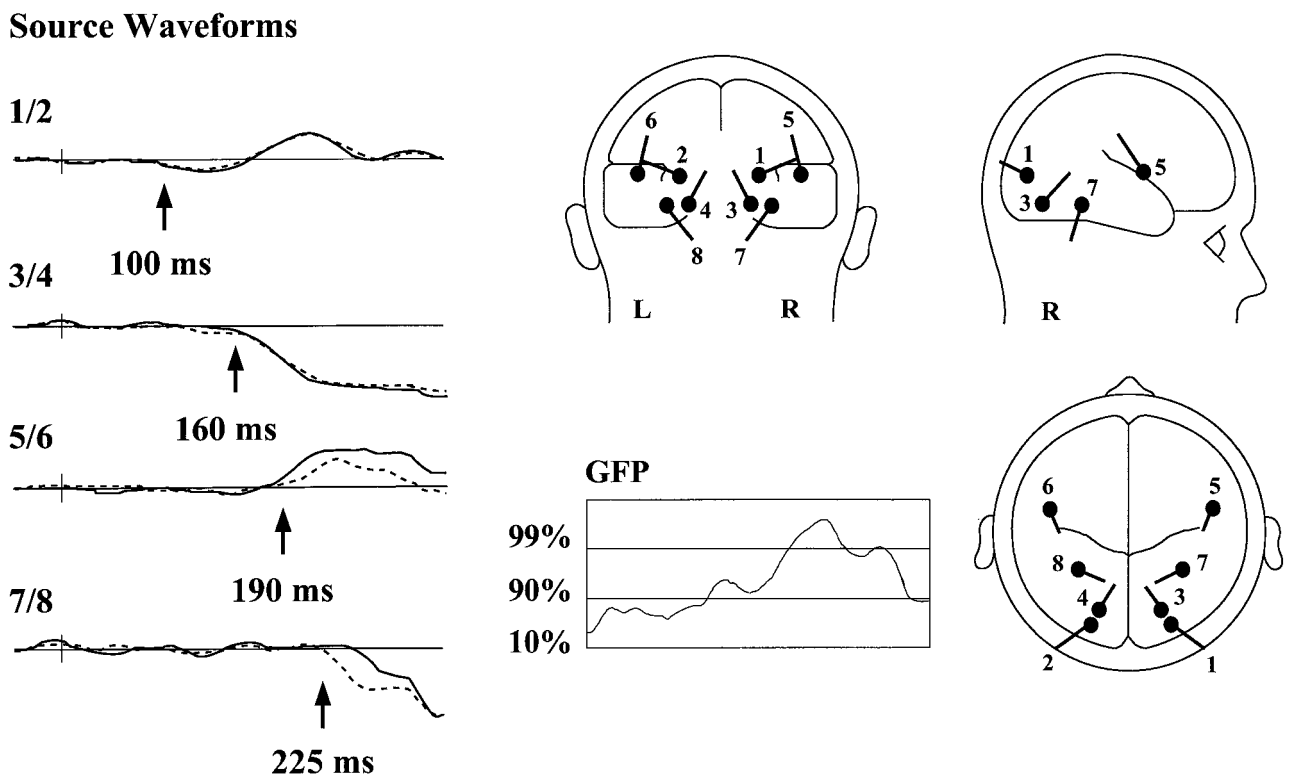

Figure 8.

Eight-dipole model of the attentional difference wave elicited by the standard stimuli. Left column shows time-varying source waveforms for each of the four dipole pairs, starting 40 ms prior to stimulus onset and lasting through 330 ms poststimulus. Dashed line corresponds to the right hemisphere and solid line to the left hemisphere. This model explained 98.6% of the variance in the difference wave distribution between 100 and 330 ms poststimulus. The central graph shows the magnitude of the goodness-of-fit parameter (GFP), the inverse of the residual variance, over time. Data are displayed with negative polarity above the baseline.

for each of the dipoles included in the final models for the standard and target stimuli. Note the high degree of similarity between the two models in the dipole locations and orientations.

Figure 10 illustrates the close correspondence between the observed and modelled scalp topographies of the attentional difference waves for the standard (top two rows) and target (bottom two rows) stimuli at four separate latencies. By referring back to the source waveforms in Figure 8, note that dipoles 1 and 2 were the only ones active at 130 ms; dipoles 3 and 4 had become active by 185 ms; the first six sources contributed to each of the models at 225 ms; and by 300 ms all eight sources were active.

Anatomical localization of group modelled sources

To obtain an estimate of the average location of the dipoles derived from the grand average difference waves for the standard stimuli (Fig. 8), the three-dimensional coordinates of each dipole were projected onto MRI scans (Fig. 11A) and transformed into Talairach and Tournoux [1988] coordinates (see Methods).[4] The coordinates of dipoles 1 and 2 placed these sources in the extrastriate cortex of the medial occipital gyrus, within Brodmann's area 18 (Table IV). The second pair of sources (dipoles 3 and 4) was located in Brodmann's area 19 in the vicinity of the collateral sulcus that separates the lingual and fusiform gyri; that is, ventral, anterior and medial with respect to the first dipole pair. As for dipoles 5 and 6, their coordinates corresponded to Brodmann's area 6, in inferior premotor cortex. Finally, dipoles 7 and 8 were located more anteriorly in the fusiform gyrus, in the ventral aspect of the

[4] Coregistration of the spherical coordinates of BESA and the non-spherical coordinates of each subject's MRI introduces some anatomical "blurring" associated with differences between subjects in brain length and degree of "roundness". To estimate the magnitude of this "blurring", we calculated the distance between the posterior perimeter of the BESA sphere and the occipital pole for each of the 6 subjects for whom we had MRIs. The average distance was 8 (±5) mm.

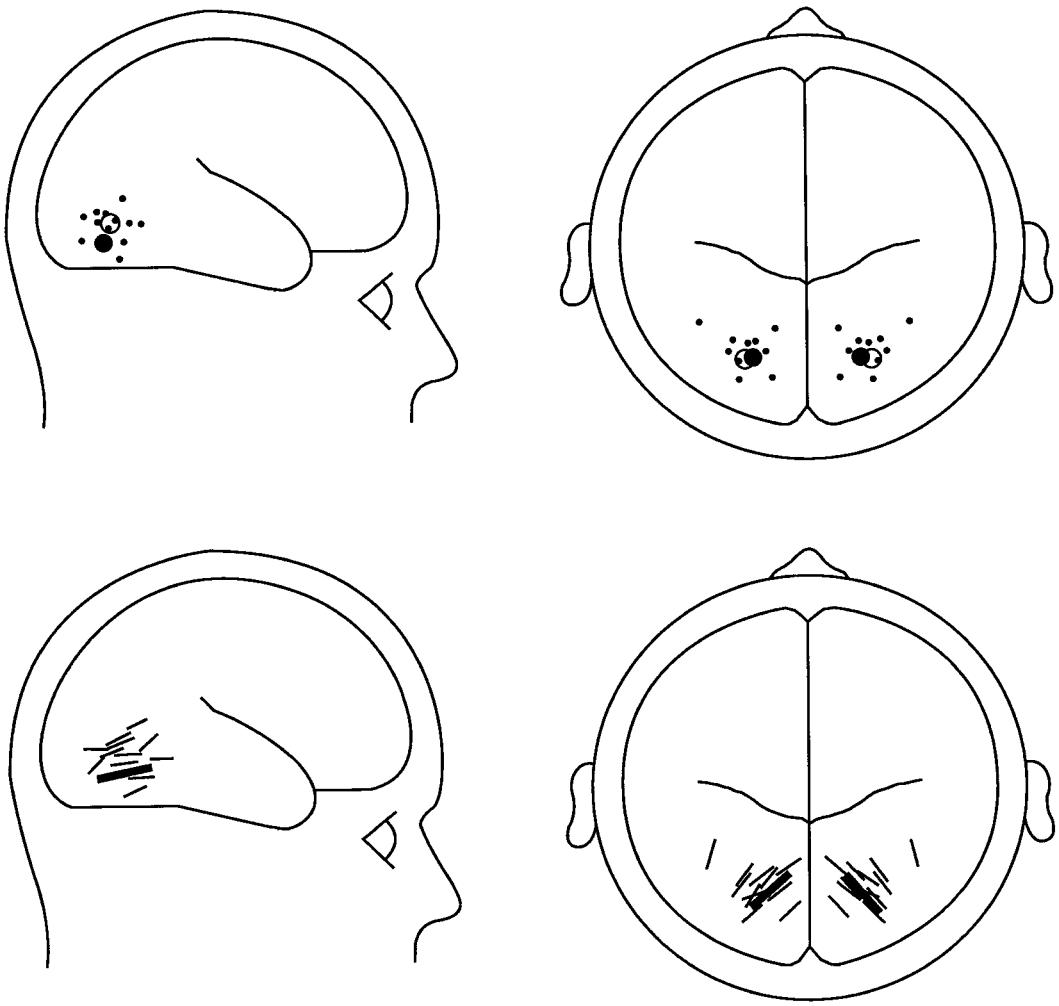

Figure 9.
Sagittal (**left**) and axial (**right**) views of the locations (**top**) and orientations (**bottom**) of the individually fitted dipolar sources that account for the initial phase of the SN (160–215 ms) in 12 separate subjects. Large outlined dots show the average location of these dipolar sources across the 12 individual subjects. Large solid dots and bars represent the location and orientation, respectively, of dipoles 3 and 4 in the eight-dipole model of the attentional difference wave depicted in Figure 8.

temporal lobe within Brodmann's area 37. Table IV gives the group mean values of each dipole location in Talairach and Tournoux [1988] coordinates, which are depicted in Figure 11B.

DISCUSSION

The present ERP recordings provided a spatio-temporal picture of color-selective attentional processing in multiple cortical regions. The initial evoked activity reflected in the C1 component at 50–90 ms after stimulus onset was not affected by attention. Beginning at about 100 ms, however, a series of attention-sensitive ERP components emerged that were localized to specific cortical areas by inverse dipole modelling and projection of the model dipoles onto co-registered MRI images. This modelling procedure indicated that color-based attentional selection took place in the region of dorsal extrastriate area 18 beginning at about 100 ms poststimulus; in the region of ventral area 19, near the collateral sulcus, beginning at about 160 ms; in the region of premotor area 6 beginning at about 190 ms; and in the region of the fusiform gyrus, area 37, beginning at about 240 ms. The overlapping waveforms corresponding to these four sources indicated that selective processing of stimuli of the attended color began at specific latencies in the different cortical areas but continued in parallel over a period of hundreds of milliseconds.

TABLE III. Locations and orientations of the eight dipoles in the group model of the attentional difference waves, expressed in the spherical coordinates of the Brain Electrical Source Analysis (BESA) program*

	Standard stimuli						
	Location (mm)				Orientation (°)		
	Eccentricity	M/L	A/P	S/I	Theta	Phi	Strength (μVeff)
Dipole 1	64.3	24.5	−59	10.1	81	−67	0.15
Dipole 2	64.3	−25	−59	10.1	−81	67.3	0.14
Dipole 3	53	19.1	−49	−7.4	98	−69	0.53
Dipole 4	53	−19	−49	−7.4	−98	68.6	0.50
Dipole 5	53.7	50.4	14.5	11.6	77.5	16	0.29
Dipole 6	53.7	−50	14.5	11.6	−78	−16	0.14
Dipole 7	41.2	32.7	−24	−9	103	−36	0.28
Dipole 8	41.2	−33	−24	−9	−103	35.7	0.32
	Target stimuli						
	Location (mm)				Orientation (°)		
	Eccentricity	M/L	A/P	S/I	Theta	Phi	Strength (μVeff)
Dipole 1	67.3	32	−58	10.6	74.8	−61	0.35
Dipole 2	67.3	−32	−58	10.6	−75	61.3	0.33
Dipole 3	52.4	19	−48	−6.9	−23	−59	1.13
Dipole 4	52.4	−19	−48	−6.9	22.8	59	1.27
Dipole 5	54.3	50	12.4	17.1	−47	74.1	0.90
Dipole 6	54.3	−50	12.4	17.1	46.5	−74	0.78
Dipole 7	48.2	28.3	−38	−7.8	−101	−11	1.18
Dipole 8	48.2	−28	−38	−7.8	101	10.8	1.14

* Cortical surface is approximately at 70 mm. Theta and phi as in Table I. Strength refers to the mean power averaged over the 100–328 ms analysis period.

It is well known that inverse source localization methods such as BESA do not yield unique solutions and can only provide approximate localizations of "centroids" of neural activity. However, the validity of inverse source calculations can be greatly enhanced by applying constraints derived from considerations of neuroanatomy and activation patterns revealed by blood-flow neuroimaging [Dale and Sereno, 1993; Heinze et al., 1994]. In the present case, the validity of the four-component dipole model was supported by a close correspondence between the calculated dipole positions and the Talairach coordinates of the color-specific cortical areas that were reported in previous neuroimaging studies (Fig. 11B, discussed below). It should be emphasized that this correspondence was achieved even though the present dipole model was obtained following the objective sequential fitting procedure described in the Results, without taking into account the prior neuroimaging data. It should also be noted that this dipole model was closely replicated in separate analyses of the standard and target ERPs, indicating that the attention-sensitive components were present with adequate signal-to-noise ratios in the attentional difference waveforms.

Early evoked cortical activity

The earliest deflection evoked by the checkerboard stimuli (the C1 wave) had an onset of approximately 50 ms and a sharply focused midline occipital scalp distribution. Both the amplitude and the topographical distribution of this component varied as a function of stimulus wavelength, with red checks evoking a larger and earlier response than blue checks over a relatively more inferior region of the scalp. Based on retinotopic mapping studies, several investigators have proposed that the C1 evoked by pattern-onset stimuli in humans is largely generated in primary visual cortex [Butler et al., 1987; Bodis-Wollner et al., 1992; Clark et al., 1995; Jeffreys and Axford, 1972]. With the foveally centered

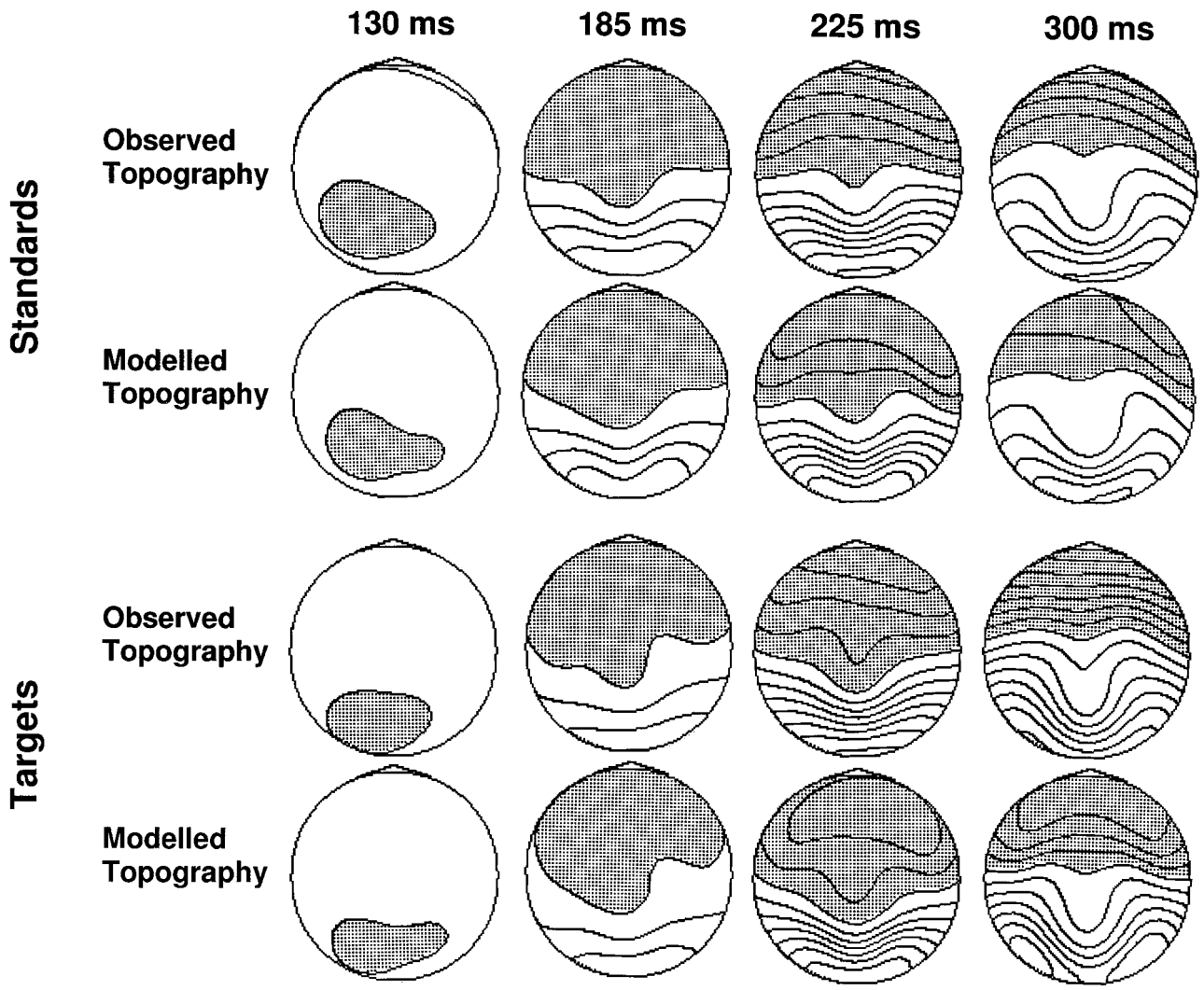

Figure 10.
Topographical maps of the observed and modelled voltage distributions of the standard (**top two rows**) and target (**bottom two rows**) difference waves at four successive latencies. Coordinates for standard and target dipole models are given in Table III.

stimuli used in this study, however, it would be difficult to distinguish between contributions to C1 from striate (V1) and extrastriate (V2, V3) cortical areas. In any case, an attempt to decompose the C1 into its respective sources through dipole analysis is beyond the scope of this paper.

In contrast to its color sensitivity, the C1 was unaffected in amplitude or distribution by the attentional manipulation. A similar lack of attentional sensitivity for the initial C1 component has been observed in electrophysiological studies of spatial attention [Anllo-Vento and Hillyard, 1996; Clark and Hillyard, 1996; Gomez Gonzalez et al., 1994; Johannes et al., 1995; Mangun et al., 1993]. Although an effect of spatial attention on presumed striate cortex activity has been reported [Aine et al., 1995], this modulation occurred at 150 ms, well after the point of initial afference, suggesting reactivation of striate cortex due to feedback from higher visual areas. PET studies of selective attention to various features of a stimulus, including color and location, have similarly failed to observe any changes in striate activity as a function of attention [Corbetta et al., 1990, 1991; Heinze et al., 1994]. Thus, in the present study, the absence of attentional modulation for the C1 wave provides further evidence that early sensory processing in the primary visual

TABLE IV. Average three-dimensional locations of the dipoles in the BESA model of the attentional difference wave for the standard stimuli, expressed in coordinates of the Talairach and Tournoux [1988] atlas

	Medial-lateral	Anterior-posterior	Superior-inferior
Dipole 1	22.3 (0.6)[a]	−83.0 (1.6)	13.5 (5.0)
Dipole 2	−27.2 (1.2)	−82.3 (1.2)	13.2 (3.8)
Dipole 3	17.7 (0.7)	−72.7 (1.9)	−3.8 (4.3)
Dipole 4	−21.2 (0.8)	−72.7 (1.7)	−5.5 (3.7)
Dipole 5	49.0 (0.7)	−7.2 (1.6)	12.8 (2.7)
Dipole 6	−52.7 (0.9)	−8.3 (1.6)	11.0 (1.6)
Dipole 7	31.2 (0.6)	−46.7 (2.1)	−10.0 (2.7)
Dipole 8	−34.8 (0.7)	−47.0 (2.0)	−7.2 (2.4)

[a] Values in parenthesis are standard errors of the mean. All values in millimeters.

cortex of humans is not sensitive to the relevance of a stimulus.

Attentional modulation of color processing in extrastriate cortex

Attentional modulation of color processing was first apparent at 100 ms following stimulus onset in the form of a positive difference wave (PD130) that was localized by dipole modelling to a region of the medial occipital gyrus included within Brodmann's area 18. However, given the relatively low proportion of variance (82%) accounted for by the dipole fit of the PD130, its localization can only be regarded as approximate. Based on recent parcellations of human visual cortex using fMRI [DeYoe et al., 1996; Sereno et al., 1995; Tootell et al., 1996], the general region of PD130 origin may correspond to dorsal extrastriate visual areas V2, V3, or V3a.

In a PET study of selective attention to various stimulus features, Corbetta and his colleagues [1990, 1991] identified several loci in dorsolateral occipital cortex that were modulated by attending selectively to the color of the stimulus array. While the Talairach coordinates of the foci of PET activation were located approximately 1.5 cm anterior to those obtained for the PD130 (dipoles 1 and 2) in this study (see Fig. 11B), this difference is within the range of intersubject variability observed in both functional [Clark et al., 1996; Lueck et al., 1989; Steinmetz et al., 1991; Watson et al., 1993] and anatomical [Rajkowska and Goldman-Rakic, 1995; Stensaas et al., 1974] studies of human cortex. As in the study of Corbetta et al. [1991], in which the dorsolateral activations were more pronounced over the left hemisphere, in the present experiment there was a clear trend towards greater PD130 amplitudes over the left hemisphere (see Figs. 5–8), although this asymmetry failed to reach statistical significance. Corbetta et al. [1991] interpreted their dorsolateral occipital activation as possibly reflecting "a further stage for color processing beyond the collateral sulcus," but this interpretation is at odds with the timing evidence obtained in the present study in which the dorsolateral PD130 actually preceded the SN component localized to the collateral sulcus by some 40 to 50 ms. Moreover, there is increasing evidence that successive stages of feature processing are carried out along the occipitotemporal pathway, rather than from ventral to more dorsal occipital regions [Allison et al., 1994; Martin et al., 1995]. A more plausible explanation would assume that the modelled PD130 sources (dipoles 1 and 2) correspond to the dorsal occipital activations reported by Corbetta et al. [1990, 1991] and that these attention effects represent a very early stage of color-selective processing.[5] In this regard, Gulyas et al. [1994] observed a similarly localized activation in a PET study of form discrimination based on color cues (see Fig. 11B).

The PD130 attention effect observed in this experiment is, to our knowledge, the earliest color-based attention effect that has been characterized in the literature, although preliminary findings of a similar color-selective modulation have been reported previously [Mangun and Hillyard, 1995]. This early positivity was of low amplitude and became significant only when ERPs were averaged over a large number of trials. Although the PD130 was elicited during the latency range of the evoked P1 wave, it seems unlikely that it represents a simple amplitude modulation of the P1 generator itself, given that the scalp distribution of the P1 (Fig. 2) was situated well inferior to that of the PD130 (Fig. 5). It is unclear at present whether the PD130 color-attention effect is related to the P1 amplitude modulation that is characteristic of visual-spatial attention. Several studies have carried out inverse dipole modelling of the P1 spatial attention effect using stimuli in the superior visual fields, and its dipolar sources were localized to ventral extrastriate

[5] It should be noted that in the present study the subjects always attended to color and that the resulting ERP attention effects reflect the selective processing of stimulus of a given color. This differs from the design of previous PET studies (e.g., Corbetta et al., 1991), which examined changes in cerebral blood flow caused by attending to the dimension of color versus other feature dimensions. The correspondence between the PET and ERP localizations, however, suggests that the same color-selective cortical areas participated in both forms of attention.

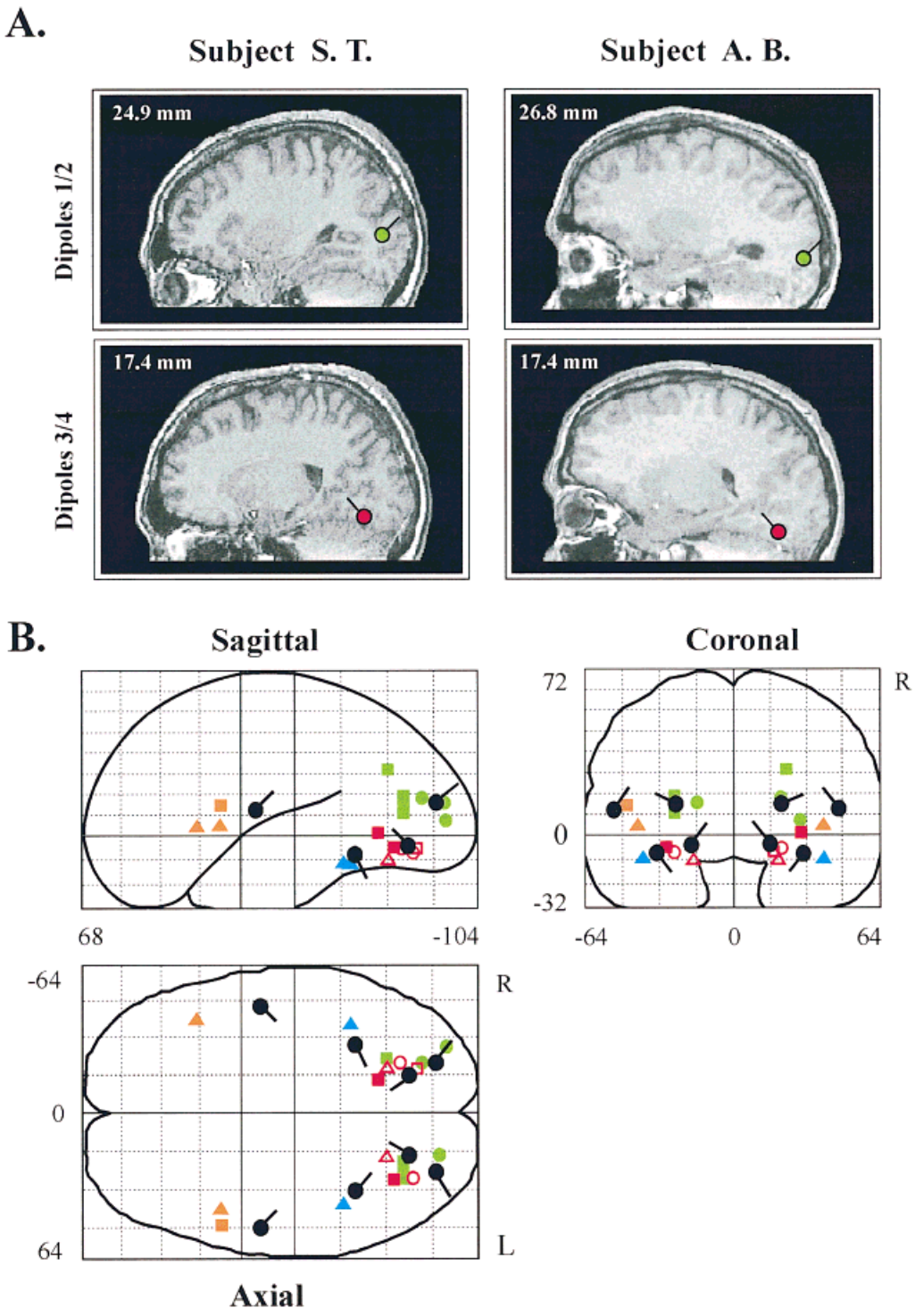

Figure 11.

A: Sagittal views of modelled dipoles 1/2 (in green) and 3/4 (in red) of the attentional difference wave, projected onto the corresponding MRI sections of two representative subjects. Distances (in mm) are lateral to the midline (x = 0) of the MRI imaging system. See Methods for details on the co-registration procedure. **B**: Sagittal, coronal, and axial views of the average brain locations of the eight dipoles in Figure 8, derived from appropriate brain sections based on the Talairach and Tournoux [1988] atlas, using the coordinates listed in Table IV (see text for details on procedure). Grids and idealized brain sections are adapted from the Statistical Parametric Mapping software. Projections of mean dipole positions are superimposed upon coordinates of PET or fMRI activations in previous studies of color-selective processing (solid squares, Corbetta et al. [1991]; outlined squares, Clark et al. [1995b]; solid circles, Gulyas et al. [1994]; outlined circles, Zeki et al. [1991]; solid triangles, Martin et al. [1995]; outlined triangles, Sakai et al. [1995]). Activations shown in green lie close to dipoles 1 and 2; in red, to dipoles 3 and 4; in orange, to dipoles 5 and 6; and, in blue, to dipoles 7 and 8.

TABLE V. Three-dimensional Talairach and Tournoux [1988] coordinates for the human homologue of area V4 in monkeys reported by previous neuroimaging studies, and for dipoles 3 and 4 of this study

Previous studies			M-L	A-P	S-I
Lueck et al. [1989]	N = 3	RH	+24	−58	−5
		LH	−27	−56	−7
Zeki et al. [1991]	N = 9	RH	+20	−66	−4
		LH	−26	−68	−8
Corbetta et al. [1991]	N = 9	RH	+21	−61	+2
		LH	−27	−65	−4
Sakai et al. [1995]	N = 6	RH	+21	−63	−10
		LH	−19	−63	−10
Clark et al. [1997]	N = 4	RH	+19	−69	−7
Present study					
Dipole 3	N = 6	RH	+18	−73	−4
Dipole 4		LH	−21	−73	−6

cortex, well inferior (by 1.8 to 2.8 cm) to those of the PD130 calculated here [Clark and Hillyard, 1996; Heinze et al., 1994; Mangun et al., 1997]. When stimuli were delivered to the inferior visual fields, however, the P1 modulation during spatial attention was modelled as having a dipolar source in dorsal occipital cortex, not far from the calculated PD130 source in the present study [Woldorff et al., 1997]. Considering that stimulus location (foveal vs. parafoveal) and type of discrimination task differed between these spatial attention studies and the present study, it is premature to speculate about whether the P1 and PD130 reflect similar stimulus selection processes.

Dipoles 3 and 4, indexing the early phase of the SN (160–250 ms), were localized to the collateral sulcus in a region that corresponds to Brodmann's area 19 and may represent the ventral portion of area V4 in humans [see below]. Two previous VEP studies of color processing that used dipole modelling techniques [Buchner et al., 1994; Plendl et al., 1993] obtained comparable dipolar sources that were interpreted as reflecting activity in human area V4. These sources had peak amplitudes between 130 and160 ms poststimulus and were inferior and anterior to dipoles representing earlier components of the VEP waveform. It should be noted, however, that VEP amplitudes in these earlier studies were comparable when evoked by colored and monochrome Mondrian stimuli and thus do not provide evidence for color-specific processing. More definitive evidence of color-selective processing in the occipito-temporal region comes from a study by Allison et al. [1993], in which cortical potentials were recorded subdurally from the fusiform and lingual gyri and were found to exhibit color-specific amplitude modulations in an adaptation paradigm. In that study, the color-selective effects in the lingual and posterior fusiform gyri had median latencies between 180 and 275 ms, in good correspondence with the time course of the SN in the present study.

Converging evidence regarding the localization of the principal human cortical area specialized for color processing comes from a series of PET studies that investigated cortical activation patterns during passive viewing of color vs. other stimulus features. Zeki and his colleagues identified a region in the lingual and fusiform gyri of extrastriate cortex that was selectively activated by color, as opposed to monochrome [Lueck et al., 1989] or moving [Zeki et al., 1991] stimuli. A very similar brain location was activated in the study of Corbetta et al. [1990, 1991] in which subjects paid attention to the color of a multidimensional stimulus array. More recently, an fMRI study of color aftereffects [Sakai et al., 1995] revealed consistent loci of activation in the posterior fusiform gyrus. Likewise, Clark et al. [1997] identified areas of the lingual and fusiform gyri that showed increased activation when the color of human faces, rather than their identity, was the feature to be attended. Table V and Figure 11B show the Talairach coordinates for the centers of activation in the studies discussed above in comparison with those of dipoles 3 and 4 in the present study. There is striking consistency across studies in the location of this color-sensitive area of the ventral occipital lobe, despite differences in stimulus parameters and imaging methodologies. Moreover, there was also good consistency in the location of dipoles 3 and 4 across the individual subjects that participated in this study (Fig. 10). It would seem likely that this area of the fusiform gyrus represents the human homolog of area V4 in the macaque, although this conclusion has been questioned by Cowey and his colleagues [Heywood et al., 1992, 1995]. In sum, the present ERP findings, in conjunction with the neuroimaging studies discussed above, indicate both that color-specific information is encoded in this ventral occipital area and is modulated by attention beginning at about 160 ms poststimulus.

The next pair of dipoles in the model (dipoles 5 and 6) became active in the 190–240 ms latency range for both standard and target stimuli. These dipoles were localized to the inferior portion of premotor area 6, and their strength was three times larger for targets than for nontargets of the attended color. This component may reflect preparatory activity in motor areas when-

ever a potentially relevant stimulus is presented, with the activity being more marked when a response is actually elicited (i.e., when targets appear). This enlarged premotor activity occurred well before the final motor responses, which had a mean latency of 510 ms. The premotor dipole location roughly corresponds to areas of activation observed in PET studies of color attention [Corbetta et al., 1991] and form discrimination based on color cues [Gulyas et al., 1994] in which subjects were asked to attend to color and to respond manually to a specific stimulus (Fig.11B).

A recent PET study on the representation of upper extremity movements in humans [Stephan et al., 1995] showed increased activation in the immediate vicinity of dipoles 5 and 6 when subjects executed a complex arm movement compared to when they only prepared to make the same movement. This is analogous to the greater premotor activity observed in the present study for target trials, on which an actual movement occurred, than for non-target trials on which no button was pressed but some motor preparation may have taken place.

Dipoles 7 and 8, which corresponded to a late phase of the SN starting at 240 ms, were localized to the fusiform gyrus in Brodmann's area 37, anterior to dipoles 3 and 4. This more anterior localization of the late SN may be related to previous intracranial ERP recordings [Allison et al., 1993, 1994; Nobre et al., 1994] showing areas of subspecialization along the extent of the fusiform gyrus in humans. Those studies found that the posterior aspect of the fusiform gyrus and the adjacent lingual gyrus encoded simple features such as color, while the anterior regions represented faces, objects, or words. In line with these specializations, Martin et al. [1995] reported that generation of colors associated with line-drawings or words for various objects activated a region of the fusiform gyrus in Brodmann's area 37 that was anterior to area V4 (Fig. 11B). Thus, the present results suggest that attentional selection of stimuli based on color involves successive stages of processing in progressively more anterior regions of the ventral visual pathways.

Conclusion

The present study provides information about the timing of color-based attentional operations in cortical areas that were shown in previous neuroimaging studies to be involved in the processing of color. Because the neuroimaging techniques that were used to identify these areas have excellent spatial but poor temporal resolution, it was necessary to complement these methods with a time-sensitive technique to obtain a full picture of both spatial and temporal aspects of color-selective attention. The link between the present ERP evidence and previous neuroimaging results was provided by the remarkable correspondence between the calculated ERP dipole locations and the Talairach coordinates of the color-selective areas reported in earlier studies (Fig. 11B). Thus, the ERP difference waveforms indicated that an early attentional selection for color takes place in dorsal occipital cortex at around 100 ms. This initial effect is followed by a much more pronounced selective processing of attended color stimuli in the region of the collateral sulcus (ventral Area 19), beginning at around 160 ms. This area of the collateral sulcus has shown consistent activation by colored stimuli in several previous neuroimaging studies and appears to be a major cortical center for the coding and analysis of color information. Both ERP and neuroimaging evidence [Clark et al., 1995b; Corbetta et al., 1990, 1991] supports the hypothesis that selective attention acts to enhance the activity of neurons in this cortical region that encode stimuli of the attended color. Subsequent ERP attention effects in premotor cortex (beginning at about 190 ms) and the fusiform gyrus (beginning at about 240 ms) appear to represent motor preparatory activity and higher level color-selective processing along the ventral occipitotemporal pathway, respectively. Further studies are needed to determine the exact nature of the attentional operations that are represented by these spatiotemporal activity patterns and how they differ from attentional operations involved in the selection of other visual features and feature conjunctions.

ACKNOWLEDGMENTS

This work was supported by a Postdoctoral Fellowship from the San Diego McDonnell-Pew Center for Cognitive Neuroscience (to L.A.-V.). We thank Jonathan Hansen for software development, Theresa Rubin and Carlos Nava for experimental assistance, and Thomas Münte and two anonymous referees for helpful comments to the manuscript.

REFERENCES

Aine CJ, Supek S, George JS (1995): Temporal dynamics of visual-evoked neuromagnetic sources: Effects of stimulus parameters and selective attention. Int J Neurosci 80:79–104.

Allison T, Begleiter A, McCarthy G, Roessler E, Nobre AC, Spencer DD (1993): Electrophysiological studies of color processing in human visual cortex. Electroencephalography Clin Neurophysiol 88:343–355.

Allison T, McCarthy G, Nobre A, Puce A, Belger A (1994): Human extrastriate visual cortex and the perception of faces, words, numbers, and colors. Cerebral Cortex 4:544–554.

Anllo-Vento L, Hillyard SA (1996): Selective attention to the color and direction of moving stimuli: Electrophysiological correlates of hierarchical feature selection. Percept Psychophys 58:191–206.

Biersdorf WR (1974): Cortical evoked responses from stimulation of various regions of the visual field. Doc Ophthlmol Proc 3:247–259.

Bodis-Wollner I, Brannan JR, Nicoll J, Frkovic S, Mylin LH (1992): A short latency cortical component of the foveal VEP is revealed by hemifield stimulation. Electroencephalography Clin Neurophysiol 84:201–208.

Buchner H, Weyen U, Frackowiak RS, Romaya J, Zeki S (1994): The timing of visual evoked potential activity in human area V4. Proc Royal Soc London. Series B: Biol Sci 257:99–104.

Butler SR, Georgiou GA, Glass A, Hancox RJ, Hopper JM, Smith KR (1987): Cortical generators of the CI component of the pattern-onset visual evoked potential. Electroencephalography Clin Neurophysiol 68:256–267.

Clark VP (1993): Localization and identification of functional regions within the human visual system. Doctoral dissertation. University of California, San Diego.

Clark VP, Hillyard SA (1996): Spatial selective attention affects early extrastriate but not striate components of the visual evoked potential. J Cogn Neurosci 8:387–402.

Clark VP, Fan S, Hillyard SA (1995): Identification of early visual evoked potential generators by retinotopic and topographic analyses. Human Brain Mapp 2:170–187.

Clark VP, Parasuraman R, Keil K, Kulanski R, Fannon S, Maisog JM, Ungerleider LG, Haxby JV (1997): Selective attention to face identity and color studied with fMRI. Human Brain Mapp 5:293–297.

Clark VP, Keil K, Maisog JM, Courtney S, Ungerleider LG, Haxby JV (1996): Functional magnetic resonance imaging of human visual cortex during face matching: A comparison with positron emission tomography. NeuroImage 4:1–15.

Corbetta M, Miezin FM, Dobmeyer S, Shulman GL, Petersen SE (1990): Attentional modulation of neural processing of shape, color, and velocity in humans. Science 248:1556–1559.

Corbetta M, Miezin FM, Dobmeyer S, Shulman GL, Petersen SE (1991): Selective and divided attention during visual discriminations of shape, color, and speed: Functional anatomy by positron emission tomography. J Neurosci 11:2383–2402.

Dale AM, Sereno MI (1993): Improved localization of cortical activity by combining EEG and MEG with MRI cortical surface reconstruction: A linear approach. J Cogn Neurosci 5:162–176.

Damasio A, Yamada T, Damasio H, Corbett J, McKee J (1980): Central achromatopsia: behavioral, anatomic, and physiologic aspects. Neurology 30:1064–1071.

Damasio, H (1995): Human Brain Anatomy in Computerized Images. New York: Oxford University Press.

DeYoe EA, Carman GJ, Bandettini P, Glickman S, Wieser J, Cox R, Miller D, Neitz J (1996): Mapping striate and extrastriate visual areas in human cerebral cortex. Proc Natl Acad Sci U S A 93:2382–2386.

Duncan J, Humphreys G (1989): Visual search and stimulus similarity. Psychol Rev 96:433–458.

Garner WR (1987): Location and color as cuing dimensions in contingent classification. Perception Psychophys 41:202–210.

Giard MH, Perrin F, Echallier JF, Thevenet M, Froment JC, Pernier J (1994): Dissociation of temporal and frontal components in the human auditory N1 wave: A scalp current density and dipole model analysis. Electroencephalography Clin Neurophysiol 92: 238–252.

Gulyas B, Heywood CA, Popplewell DA, Roland PE, Cowey A (1994): Visual form discrimination from color or motion cues: Functional anatomy by positron emission tomography. Proc Natl Acad Sci U S A 91:9965–9969.

Gomez Gonzalez CM, Clark VP, Fan S, Luck SJ, Hillyard SA (1994): Sources of attention-sensitive visual event-related potentials. Brain Topography 7:41–51.

Harter MR, Aine C (1984): Brain mechanisms of visual selective attention. In: Parasuraman P, Davis DR (eds): Varieties of Attention. New York: Academic Press, pp 293–321.

Harter MR, Aine C, Schroeder C (1982): Hemispheric differences in the neural processing of stimulus location and type: effects of selective attention on visual evoked potentials. Neuropsychologia 20:421–438.

Harter MR, Guido W (1980): Attention to pattern orientation: negative cortical potentials, reaction time, and the selection process. Electroencephalography Clin Neurophysiol 49:461–475.

Harter MR, Previc FH (1978): Size-specific information channels and selective attention: visual evoked potential and behavioral measures. Electroencephalography Clin Neurophysiol 45:628–640.

Heinze HJ, Mangun GR, Burchert W, Hinrichs H, Scholz M, Munte TF, Gos A, Scherg M, Johannes S, Hundeshagen, Gazzaniga MS, Hillyard SA (1994): Combined spatial and temporal imaging of brain activity during visual selective attention in humans. Nature 372:543–546.

Heslenfeld DJ, Kenemans JL, Kok A, Molenaar PCM (1997): Feature processing and attention in the human visual system: an overview. Biol Psychol 45:183–215.

Heywood CA, Gadotti A, Cowey A (1992): Cortical area V4 and its role in the perception of color. J Neurosci 12:4056–4065.

Heywood CA, Gaffan D, Cowey A (1995): Cerebral achromatopsia in monkeys. Euro J Neurosci 7:1064–1073.

Hillyard SA, Münte TF (1984): Selective attention to color and location: an analysis with event-related brain potentials. Percept Psychophys 36:185–198.

Hillyard SA, Anllo-Vento L, Clark VP, Heinze HJ, Luck SJ, Mangun GR (1996): Neuroimaging approaches to the study of visual attention: A tutorial. In: Coles M, Kramer A, Logan G (eds): Converging Operations in the Study of Visual Selective Attention. Washington, DC: American Psychological Association, pp 107–138.

Horel JA (1994): Retrieval of color and form during suppression of temporal cortex with cold. Behav Brain Res 65:165–172.

Jeffreys DA, Axford JG (1972): Source locations of pattern-specific components of human visual evoked potentials. I: Components of striate cortical origin. Exp Brain Res 16:1–21.

Johannes S, Münte T, Heinze HJ, Mangun GR (1995): Luminance and spatial attention effects on early visual processing. Brain Research. Cogn Brain Res 2:189–205.

Karayanidis F, Michie PT (1996): Frontal processing negativity in a visual selective attention task. Electroencephalography Clin Neurophysiol 99:38–56.

Kenemans JL, Kok A, Smulders FT (1993):Event-related potentials to conjunctions of spatial frequency and orientation as a function of stimulus parameters and response requirements. Electroencephalography Clin Neurophysiol 88:51–63.

Komatsu H, Ideura Y, Kaji S, Yamane S (1992): Color selectivity of neurons in the inferior temporal cortex of the awake macaque monkey. J Neurosci 12:408–424.

Livingstone MS, Hubel DH (1984): Anatomy and physiology of a color system in the primate visual cortex. J Neurosci 4:309–356.

Lueck CJ, Zeki S, Friston KJ, Deiber MP, Cope P, Cunningham VJ, Lammertsma AA, Kennard C, Frackowiak RS (1989): The colour centre in the cerebral cortex of man. Nature 340:386–389.

Mangun GR, Hillyard SA (1990): Allocation of visual attention to spatial locations: Tradeoff functions for event-related brain potentials and detection performance. Perception Psychophys 47:532–550.

Mangun GR, Hillyard SA (1995): Mechanisms and models of selective attention. In: Rugg MD, Coles MGH (eds): Electrophysiology of Mind. Event-Related Brain Potentials and Cognition. Oxford, UK: Oxford University Press, pp 40–85.

Mangun GR, Hillyard SA, Luck SJ (1993): Electrocortical substrates of visual selective attention. In: Meyer DE, Kornblum S (eds): Attention and Performance 14: Synergies in Experimental Psychology, Artificial Intelligence, and Cognitive Neuroscience. Cambridge, MA: MIT Press, pp 219–243.

Mangun GR, Hopfinger JB, Kussmaul CL, Fletcher EM, Heinze H-J (1997): Covariations in ERP and PET measures of spatial selective attention in human extrastriate visual cortex. Human Brain Mapp 5:273–279.

Martin A, Haxby JV, Lalonde FM, Wiggs CL, Ungerleider LG (1995): Discrete cortical regions associated with knowledge of color and knowledge of action. Science 270:102–105.

McCarthy G, Wood CC (1985): Scalp distributions of event-related potentials: an ambiguity associated with analysis of variance models. Electroencephalography Clin Neurophysiol 62:203–208.

Nobre AC, Allison T, McCarthy G (1994): Word recognition in the human inferior temporal lobe. Nature 372:260–263.

Nunez PL (1981): Electric Fields of the Human Brain. New York: Oxford University Press.

Pantev C, Bertrand O, Eulitz C, Verkindt C, Hampson S, Schuriere G, Elbert T (1995): Specific tonotopic organizations of different areas of the human auditory cortex revealed by simultaneous magnetic and electric recordings. Electroencephalography Clin Neurophysiol 94:26–40.

Perrin F, Pernier J, Bertrand O, Echallier JF (1989): Spherical splines for scalp potential and current density mapping. Electroencephalography Clin Neurophysiol 72:184–187.

Plendl H, Paulus W, Roberts IG, Botzel K, Towell A, Pitman JR, Scherg M, Halliday AM (1993): The time course and location of cerebral evoked activity associated with the processing of colour stimuli in man. Neurosci Lett 150:9–12.

Previc FH, Harter MR (1982): Electrophysiological and behavioral indicants of selective attention to multifeature gratings. Perception Psychophys 32:465–472.

Rajkowska G, Goldman-Rakic PS (1995): Cytoarchitectonic definition of prefrontal areas in the normal human cortex: II. Variability in locations of areas 9 and 46 and relationship to the Talairach Coordinate System. Cerebral Cortex 5:323–337.

Rugg MD, Milner AD, Lines CR, Phalp R (1987): Modulation of visual event-related potentials by spatial and non-spatial visual selective attention. Neuropsychologia 25:85–96.

Sakai K, Watanabe E, Onodera Y, Uchida I, Kato H, Yamamoto E, Koizumi H, Miyashita Y (1995): Functional mapping of the human colour centre with echo-planar magnetic resonance imaging. Proc Royal Soc London. Series B: Biol Sci 261:89–98.

Scherg M (1990): Fundamentals of dipole source analysis. In: Grandori F, Hoke M, Roman GL (eds): Auditory Evoked Magnetic Fields and Electric Potentials. Basel: Karger, pp 40–69.

Schein SJ, Desimone R (1990): Spectral properties of V4 neurons in the macaque. J Neurosci 10:3369–3389.

Schiller PH, Logothetis NK, Charles ER (1990): Role of the color-opponent and broad-band channels in vision. Vis Neurosci 5:321–346.

Sereno MI, Dale AM, Reppas JB, Kwong KK, Belliveau JW, Brady TJ, Rosen BR, Tootell RB (1995): Borders of multiple visual areas in humans revealed by functional magnetic resonance imaging. Science 268:889–893.

Simpson GV, Foxe JJ, Vaughan HG, Mehta AD, Schroeder CE (1995): Integration of electrophysiological source analyses, MRI and animal models in the study of visual processing and attention. Electroencephalography Clin Neurophysiol Suppl 44:76–92.

Smid HGOM, Heinze H-J (1997): An electrophysiological study of the selection of the color and shape of alphanumeric characters in response choice. Biol Psychol 44:161–185.

Steinmetz H, Seitz RJ (1991): Functional anatomy of language processing: neuroimaging and the problem of individual variability. Neuropsychologia 29:1149–1161.

Stensaas SS, Eddington DK, Dobelle WH (1974): The topography and variability of the primary visual cortex in man. J Neurosurg 40:747–755.

Stephan KM, Fink GR, Passingham RE, Silbersweig D, Ceballos-Bauman AO, Frith DC, Frackowiak RS (1995): Functional anatomy of the mental representation of upper extremity movements in healthy subjects. J Neurophysiol 73:373–386.

Talairach J, Tournoux P (1988): Co-planar Stereotaxic Atlas of the Human Brain. Sttutgart: Thieme.

Theeuwes J (1990): Perceptual selectivity is task dependent: evidence from selective search. Acta Psychologica 74:81–99.

Theeuwes J (1996): Perceptual selectivity for color and form: On the nature of the interference effect. In: Coles M, Kramer A, Logan G (eds): Converging Operations in the Study of Visual Selective Attention. Washington, DC: American Psychological Association, pp 297–314.

Tootell, RBH, Dale, AM, Sereno, MI, Malach, R (1996): New images from human visual cortex. Trends Neurosci 19:481–489.

Towle VL, Bolaños J, Suarez D, Tan K, Grzeszczuk R, Levin DN, Cakmur SA, Spire J-P (1993): The spatial location of EEG electrodes: locating the best-fitting sphere relative to cortical anatomy. Electroencephalography Clin Neurophysiol 86:1–6.

Treisman AM, Gelade G (1980): A feature-integration theory of attention. Cogn Psychol 12:97–136.

Vasey MW, Thayer JF (1987): The continuing problem of false positives in repeated measures ANOVA in psychophysiology: A multivariate solution. Psychophysiology 24:479–486.

Watson JD, Myers R, Frackowiak RS, Hajnal JV, Woods RP, Mazziotta JC, Shipp S, Zeki S (1993): Area V5 of the human brain: evidence from a combined study using positron emission tomography and magnetic resonance imaging. Cerebral Cortex 3:79–94.

Wijers AA, Mulder G, Okita T, Mulder LJ, Scheffers MK (1989): Attention to color: an analysis of selection, controlled search, and motor activation, using event-related potentials. Psychophysiology 26:89–109.

Woldorff MG (1993): Distortion of ERP averages due to overlap from temporally adjacent ERPs: analysis and correction. Psychophysiology 30:98–119.

Woldorff MG, Fox PT, Matzke M, Lancaster L, Veeraswamy S, Zamarripa F, Seabolt M, Glass T, Gao JH, Martin CC, Jerabek P (1997): Retinotopic organization of early visual spatial attention effects as revealed by PET and ERP data. Human Brain Mapp 5:280–286.

Zani A, Proverbio AM (1995): ERP signs of early selective attention effects to check size. Electroencephalography Clin Neurophysiol 95:277–292.

Zeki S (1990): A century of cerebral achromatopsia. Brain 113:1721–1777.

Zeki S, Watson JD, Lueck CJ, Friston KJ, Kennard C, Frackowiak RS (1991): A direct demonstration of functional specialization in human visual cortex. J Neurosci 11:641–649.